Western University
Scholarship@Western

2009

Evaluation of Cerebral Lateral Ventricular Enlargement Derived from Magnetic Resonance Imaging: A Candidate Biomarker of Alzheimer Disease Progression in Vivo

Sean M. Nestor

Follow this and additional works at: https://ir.lib.uwo.ca/digitizedtheses

Evaluation of Cerebral Lateral Ventricular Enlargement Derived from Magnetic Resonance Imaging: A Candidate Biomarker of Alzheimer Disease Progression *in Vivo*

(Spine Title: Ventricular Enlargement in MCI and AD)

(Thesis Format: Integrated Article)

by

Sean M. <u>Nestor</u>

Graduate Program in Medical Biophysics

A thesis submitted in partial fulfillment
Of the requirements for the degree of
Master of Science

/

School of Graduate and Postdoctoral Studies
The University of Western Ontario
London, Ontario
June 2009

ABSTRACT

Alzheimer disease (AD) is the most common form of dementia and has grievous mortality rates. Measuring brain volumes from structural magnetic resonance images (MRI) may be useful for illuminating disease progression. The goal of this thesis was to (1) help refine a novel technique used to segment the lateral cerebral ventricles from MRI, (2) validate this tool, and determine group-wise differences between normal elderly controls (NEC) and subjects with mild cognitive impairment (MCI) and AD and (3) determine the number of subjects necessary to detect a 20 percent change from the natural history of ventricular enlargement with respect to genotype. Three dimensional T_1-weighted MRI and cognitive measures were acquired from 504 subjects (NEC $n =$ 152, MCI $n = 247$ and AD $n = 105$) participating in the multi-centre Alzheimer's Disease Neuroimaging Initiative. Cerebral ventricular volume was quantified at baseline and after six months. For secondary analyses, all groups were dichotomized for Apolipoprotein E genotype based on the presence of an ε4 polymorphism. The AD group had greater ventricular enlargement compared to both subjects with MCI ($P = 0.0004$) and NEC ($P <$ 0.0001), and subjects with MCI had a greater rate of ventricular enlargement compared to NEC ($P = 0.0001$). MCI subjects that progressed to clinical AD after six months had greater ventricular enlargement than stable MCI subjects ($P = 0.0270$). Ventricular enlargement was different between apolipoprotein E genotypes within the AD group ($P = 0.010$). The number of subjects required to demonstrate a 20% change in ventricular enlargement (AD: N=342, MCI: N=1180) was substantially lower than that required to demonstrate a 20% change in cognitive scores (MMSE) (AD: N=7056, MCI: N=7712). Therefore, ventricular enlargement represents a feasible short-term marker of disease progression in subjects with MCI and subjects with AD for multi-centre studies.

Keywords: magnetic resonance imaging, ventricular enlargement, mild cognitive impairment, Alzheimer disease, apolipoprotein E, Alzheimer's disease neuroimaging initiative

Chapter 1

INTRODUCTION

The work in this thesis uses high resolution (256 x 256 in-plane matrix and 26 cm field of view) magnetic resonance imaging (MRI) and a novel segmentation tool called Brain Ventricle Quantification (BVQ), Cedara Software, for the purpose of characterizing Alzheimer disease (AD) progression and improving the study of AD.

As such, this introductory chapter provides a framework for understanding the motivation, impact, and research methods presented in the subsequent chapters. Two principal subjects are described. The first is a description of AD neuropathology and clinical characterization. The second topic highlights imaging studies, in particular MRI, in the study, measurement of progression and diagnosis of AD. Neuroimaging studies of ventricular volume and the Apolipoprotien E (ApoE) gene are introduced. The basics of MRI volumetry are discussed. Finally, a description of the Alzheimer Disease Neuroimaging Initiative (ADNI) is presented.

1.1 ALZHEIMER DISEASE

1.1.1 IMPACT

Alzheimer disease is a neurodegenerative disease that is the most common cause of dementia and characterized by progressive cerebral atrophy (Fox, et al. 2000). Approximately 500,000 Canadians are afflicted with AD or a related dementia (Alzheimer's Society of Canada. January 2009). The incidence of AD increases with age and the prevalence approximately doubles every five years after the age of 60 (Mount and Downton. 2006). Given the portended increase in persons over 60 years of age, the prevalence of this disease is expected to surge on a global scale (Vas, et al. 2001). The economic costs of this scourge are estimated to be approximately 160 billion dollars (Wimo, et al. 2006). Large research efforts and resources are being allocated for the development of purported disease modifying therapies, which may arrest the disease or

prevent further progression (Small, et al. 2008). Moreover, imaging and molecular technologies are being investigated to provide a more sensitive and specific disease characterization at an earlier stage (Mosconi, et al. 2007). This characterization may facilitate an earlier diagnosis and appropriate intervention. A few available treatments for AD ameliorate cognitive symptoms for a short period (Petersen, et al. 2005, Wilcock, et al. 2000). There are currently no approved disease-modifying therapies available.

1.1.2 PATHOGENESIS

Advances in analytical methods in the mid nineteenth century allowed Wilks and colleagues to identify changes in brain structure and global atrophy as pathological features of dementia (Wilks. 1864). Further, histological staining technology in the late nineteenth century provided a means to interrogate the pathology of dementing illnesses within the neuronal environment (Graeber, et al. 1997). Alois Alzheimer in 1907, using a silver staining technique visualized the two pathological hallmarks of AD, namely the inclusions intraneuronal neurofibrillary tangles (NFTs) and extracellular senile plaques in the post-mortem brain (Moller and Graeber. 1998). This pathological characterization did not fit within the available nosological framework of dementing disorders (Berchtold and Cotman. 1998). Afterwards, Emil Kraeplin conceptualized the disease as AD in 1910. Over the next several decades, plaque and tangle pathology was studied in microscopic detail (Moller and Graeber. 1998). Histopathological descriptions of these neuronal aberrations were refined and reported as abnormal accumulations of two misfolded proteins, namely extracellular accumulation of the protein β-amyloid (Aβ) (Glenner and Wong. 1984), and intraneuronal accumulation of a hyperphosphorylated form of the microtubule-associated protein tau (Grundke-Iqbal, et al. 1986). In addition to the presence of Aβ plaques and NFTs, increased glial cell (microglia and astroglia) activation is present and significant atrophy is observed in brain regions where neuronal death has occurred (Braak and Braak. 1994), particularly in the paralimbic and medial temporal lobe (MTL) structures including the hippocampus and entorhinal cortex (Devanand, et al. 2007, Fjell, et al. 2008). According to Braak staging of AD (Braak and Braak. 1994) the pathology evolves in a lateropareital direction. Ultimately, it is the gradual neuronal dysfunction, loss of cortical structure viability and decline in synaptic connectivity which

gradually affects normal cognition, promotes loss of executive function (Jack, et al. 2008, Mosconi, et al. 2008).

1.1.3 DIAGNOSIS

Although dementia has been recognized throughout antiquity from the Greco-Roman period (Berchtold and Cotman. 1998), the first systematic clinical descriptions were ascribed by Esquirol in the mid eighteenth century (Berchtold and Cotman. 1998). A dramatic improvement in histological methods allowed Alois Alzheimer in 1907 to remark on the pathological hallmarks of AD. Over the next several decades, plaque and tangle pathology were extensively evaluated (Grundke-Iqbal, et al. 1986, Schmechel, et al. 1993). The conceptualization of AD evolved over the next century and in 1984 the National Institute of Neurological and Communicative Disorders and Stroke and the Alzheimer's Disease and Related Disorders Association (NINCDS-ADRDA) Alzheimer disease criteria were formulated to harmonize the definition of AD and are commonly used to render a diagnosis of AD (McKhann, et al. 1984). These criteria require that the presence of cognitive impairment and a suspected dementia syndrome be confirmed by neuropsychological evaluation for a clinical diagnosis of possible or probable AD. A post-mortem histopathologic confirmation is necessary for a definitive diagnosis of AD (Braak and Braak. 1994). They explicate eight cognitive domains that may be impaired in AD including: memory, language (aphasia), perceptual skills (agnosia), attention, constructive abilities, orientation, problem solving and functional abilities (McKhann, et al. 1984). A family history of AD and noticeable atrophy from serial MRI may also help to support a diagnosis of AD. The Diagnostic and Statistical Manual of Mental Disorders IV-TR is also frequently used to render a diagnosis of AD (American Psychiatric Association and American Psychiatric Association. 2000). More generally, AD impairs memory to the extent that it impedes a person's work, hobbies or social life. This and other symptoms vary widely. Other symptoms may include confusion, trouble with organizing and expressing thoughts, misplacing items, getting lost in familiar places, and changes in personality and behaviour (Shaw. 2008).The development of AD clinical criteria has improved diagnostic accuracy, but is still not ideal, with specificity varying between 76% and 88%, and sensitivity ranging between 53% and 65% (Petrovitch, et al.

2001). Neuroimaging, CSF biomarkers, and more sensitive cognitive tests may improve diagnostic accuracy for AD.

In addition to neuropsychological evaluation, certain laboratory tests are often used to rule out other causes of dementia. These tests include screening blood tests, such as syphilis serology and measures of thyroid function or vitamin B12 (Scheltens, et al. 2002). In addition, neuroimaging is an attractive approach to excluding other factors contributing to cognitive impairment including hematoma, normal pressure hydrocephalus (NPH), space occupying lesions such as tumour or stroke (Small, et al. 2008). However, the yield of laboratory tests and exclusionary neuroimaging is approximately 1 percent of all causes of dementia (Scheltens, et al. 2002). More prevalent forms of dementia include AD, vascular dementia (VD), dementia with Lewy bodies (DLB), and frontotemporal dementia (FTD). The pathological processes underpinning these dementias contribute to brain atrophy, which can be measured by neuroimaging technologies. This obviates the use of neuroimaging to support a clinical diagnosis of dementia. Imaging may provide an earlier diagnosis of AD and may facilitate earlier treatment. This is particularly useful with several purported disease modifying therapies in stage III clinical trials (U.S. National Institute of Health. May 2009). Moreover, it might be more feasible to rescue a brain with less atrophy and pathological burden via early detection. The American Academy of Neurology Practice Parameter guidelines now recommend structural neuroimaging with either a non-contrast CT or MRI scan for the assessment of patients with dementia (Knopman, et al. 2001). In addition, Dubois *et al.* have purposed new research diagnostic criteria for AD, which may provide earlier detection using episodic memory as a primary criterion supported by a panel of biomarkers, genetics and structural neuroimaging markers (Dubois, et al. 2007).

1.1.4 MILD COGNITIVE IMPAIRMENT

In 1999 Peterson and colleagues from the Mayo Clinic conceptualized the diagnostic entity of mild cognitive impairment (MCI) (Petersen, et al. 2001). This was effectively a classification for persons with objective memory impairment but who did not fulfill the clinical criteria for dementia (Petersen, et al. 2001). This is a cognitively heterogeneous group. Approximately 15% of persons with MCI convert to AD annually (Petersen, et al.

1999). One study reported 17% of persons with MCI back-converted to normal after a follow up of 3.5 years (Alexopoulos, et al. 2006). This definition was further focused by categorizing subtypes of MCI (Petersen, et al. 2001). These subtypes are representative of affected cognitive domains. The amnestic form of MCI, characterized by episodic memory impairment is typically considered preclinical AD (Petersen, et al. 2001). A diagnosis of MCI is predicated on objective memory impairment measured by neuropsychological evaluation, a memory complaint by an informant (usually citing marked memory decline over one year), normal general cognitive function, intact activities of daily living and no dementia (Winblad, et al. 2004). The viability of MCI as a diagnostic entity remains contentious. Neuroimaging and biomarkers may help illuminate the underlying pathology and identify individuals with incipient dementia.

1.2 MAGNETIC RESONANCE IMAGING STUDIES IN MCI AND AD

1.2.1 STRUCTURAL NEUROIMAGING METHODS IN AD

Structural neuroimaging techniques offer the capacity to track AD-related brain changes *in vivo*, which is critical for investigating a person with cognitive impairment. The main purposes of neuroimaging in AD have evolved from exclusionary diagnostic criteria to the detection of very early AD at a prodromal stage (MCI), predicting future decline, and differential diagnosis from other dementias (Scheltens, et al. 2002) The most commonly used structural technologies in AD include CT, PET and MRI (Mosconi, et al. 2007).

CT scanning provides high-resolution (approximately $1mm^3$ voxel size) brain images (Small, et al. 2008). Historically, structural studies in AD were performed using CT (Barron, et al. 1976, de Leon, et al. 1989a). The lateral ventricles were particularly studied using linear measurement techniques (Gado, et al. 1983). However, with the growing availability of MR scanners, flexibility of MR, non-ionising radiation and its exquisite tissue contrast, MRI principally replaced CT for structural imaging studies in MCI and AD. However, improvements in CT, over the last decade, have allowed for greater flexibility and better spatial resolution, with voxel sizes similar to clinical MRI.

In PET imaging a radiotracer is injected intravenously which emits a positron that annihilates and releases two gamma rays that travel in opposite directions. The scanner

records the gamma rays at detectors 180 degrees apart and computes the line along which the annihilation occurs to construct a PET image. Spatial resolution is 3-5 mm. One of the most widely studied PET compounds is the amyloid-binding radiotracer [^{11}C]-labelled Pittsburgh compound B (2-[4L-(methylamino)phenyl]-6-hydrobenzo-thiazole, PIB), a derivative of thioflavin-T amyloid dye that binds to amyloid-β plaques (Klunk, et al. 2004). PET studies using [^{11}C]PIB show marked cortical retention in patients with AD in comparison to normal elderly controls (Nordberg. 2004). Longitudinal follow-up studies demonstrate stable levels of [^{11}C]PIB retention despite cognitive function (Small, et al. 2008). Further investigation is required to clarify the longitudinal signature of PIB in persons with MCI and AD. Amyloid PET ligands that use fluorine-18, demonstrate similar results to PIB studies and have a sufficient half-life to potentially employ in a clinical setting (Small, et al. 2006).

MRI provides high-resolution (approximately 1 mm^3 voxel size) detail of structure, including excellent differentiation of gray matter and white matter from T$_1$-weighted clinical images. There is no ionizing radiation exposure to the subject, although surgical implants containing certain metals are exclusionary criteria for MRI. MTL regions including hippocampal atrophy measures demonstrate group-wise discrimination between healthy elderly, MCI and AD (Devanand, et al. 2007). Moreover, studies of hippocampal atrophy (Devanand, et al. 2007, Jack, et al. 2005), entorhinal cortex atrophy (Devanand, et al. 2007, Jack, et al. 2004a) and changes in the lateral ventricles (Bradley, et al. 2002, Carmichael, et al. 2007, Fleisher, et al. 2008, Giesel, et al. 2006, Jack, et al. 2004b, Schott, et al. 2005, Silbert, et al. 2003, Thompson, et al. 2004, Wang, et al. 2002) have demonstrably predicted memory decline in MCI and AD (Jack, et al. 2004a, Jack, et al. 2005). However, the specificity of these structural changes is unclear and may occur in other causes of dementia (Lehericy, et al. 2007, Scheltens, et al. 2002, Schuff and Zhu. 2007). Other voxel-wise studies have demonstrated *in vivo* progression of cortical atrophy from longitudinal MRI in persons with MCI and AD (O'Brien. 2007). These studies typically demonstrate pernicious involvement in the MTL structures with atrophy progressing laterally and projecting into the frontal lobe. The primary sensory and motor cortices are characteristically spared until the terminal stages of AD (Braak and Braak. 1994).

A combination approach using neuroimaging with other procedures that provide data on genetic risk and biomarker profiles from other tissues (for example CSF) might enhance diagnostic sensitivity and specificity.

1.2.2 INTRODUCTION TO MAGNETIC RESONANCE IMAGING

MRI uses a strong, static magnetic field (B_0) to produce a net magnetization (M) from atomic nuclei that have an odd number of protons and/or neutrons. Hydrogen nuclei or protons are abundant in fluid and body tissues of humans and are principally used for MRI. To produce a detectable MR signal, a radio frequency magnetic field (B_1) oscillating at the Larmor frequency of a given species is used to excite the nuclei in the sample. During and following excitation, the system returns to the equilibrium state after a certain period. In the classical description of signal excitation, the net magnetization vector (M_0), which is parallel to the z-axis at equilibrium, is rotated away from the z-direction towards the x-y-plane. The degree of rotation is dependent upon the length of time the B_1 field is on. When a 90 degree B_1 pulse is applied, M_0 rotates entirely into the transverse (x-y) plane, where it precesses about the main magnetic field B_0 and interacts with the RF coil to produce a signal that is recorded. Once the radio frequency (RF) pulse is turned off the system relaxes back to equilibrium and the magnitude of the detected signal decreases over time. There are several mechanisms that contribute to the loss in MR signal. First, there is an exchange of energy from individual nuclei to the lattice. This loss of energy from the spin system results in the exponential re-growth of the net magnetization vector in the z-direction. The T_1 time constant describes the length of time needed to re-establish the net magnetization vector (spin-lattice relaxation). Second, there is a loss of detectable magnetization in the transverse plane due to spin-lattice relaxation, a loss of spin phase coherence due to local magnetic field variations seen by individual spins, and a loss of phase coherence due to the exchange of energy between spins. The exponential rate of signal loss in the transverse plane due to spin-lattice relaxation and the exchange of energy between spins (*spin-spin* relaxation) is described by the time constant T_2, and the time constant T_2^* additionally describes the effects of magnetic field non-uniformities experienced by the sample

Following excitation, spins will lose phase coherence due to inherent differences in magnetic field within the sample, and due to the exchange of energy between nuclei. To eliminate the effects of inhomogeneous magnetic fields, and allow the measurement of the intrinsic T_2 time constant associated with a sample, spins must be refocused in the transverse plane. Such refocusing can be achieved by the application of a 180° pulse in the transverse plane at some time after the excitation pulse, time to echo (TE)/2. The effect of this 180° pulse is to rotate spins about the transversal plane. The result is that spins that had accumulated greater phase in the transverse plane than the ensemble average of spins (because they were experiencing a larger magnetic field) will now be behind by the same amount. Similarly, spins that accumulated less phase than the ensemble average will be ahead by the same amount. Following a second time interval (TE/2) a refocusing of the spins will occur to form a new net magnetization, as the more quickly precessing spins catch up with the slower spins, at TE. This refocusing will generate a re-growth of the MR signal called a spin-echo. This refocusing or spin-echo can be performed multiple times and the amplitude of the echo signals can be fitted to an exponential T_2 decay curve to determine the T_2 time constant of a sample.

The precession of M about B_0 following excitation induces a voltage in a surrounding RF coil (inductor). The magnitude of the voltage is greatest when there is the greatest component of M in the transverse (x-y) plane and perpendicular to the plane of the RF coil (that is, immediately after RF pulse is applied) and least when M is nearly parallel to B_0. The induced signal or free induction decay (FID) will change in amplitude and phase as a function of time. This variation in time reflects the local environments of the molecule of interest. That is, different molecular environments will influence the rate at which the spins precess, dephase, and relax. These properties will directly affect the signal detected by the RF coil.

In order to spatially locate the signal from the object being scanned, a magnetic field gradient is used. The magnetic field gradient is superimposed on the homogenous magnetic field (B_0) causing the magnetic field experienced by the nuclei in the sample to vary linearly along an axis of the object, provided the gradient is linear. As the magnetic field varies, so does the precession frequency (or Larmor frequency) of the nuclei.

Therefore the position of the spins is directly related to precession frequency (frequency encode direction). By varying the magnitude of the gradients applied in a predefined manner (phase encode direction), the position of the nuclei in the sample can be decoded through the use of the Fourier transform. In this way, an image can be generated from the acquired time domain signal followed by a discrete 2D or 3D Fourier transformation. The signal produced in an MR experiment can be influenced by a myriad of physical and biochemical features; these factors include molecular structure, flow, diffusion, density, magnetic environment and nuclear mobility. By exploiting these properties, tissue types can be readily distinguished and structural and functional details may be rendered.

The three most common contrast mechanisms are based on tissue differences in T_1 and T_2 relaxation time constants, and proton density (PD). To generate contrast between tissue types based on these magnetic properties "weighted" imaging may be performed; hence, one collects T_1-weighted, T_2-weighted, and PD-weighted images. For instance, in spin-echo pulse sequences (as described above) relaxation weighting are obtained by varying the timing parameters, echo time (TE) and repetition time (TR), during acquisition of the MR signal. Specifically, T_1-weighted images can be acquired using a short TE and TR, PD weighted images can be acquired using a short TE and long TR, and T_2-weighted images can be acquired using a long TE and TR.

T_1-weighted images can also be acquired using faster MR imaging methods such as the Fast Low-Angle Shot (FLASH) imaging (Scheffler and Lehnhardt. 2003). Such pulse sequences are often used to acquire high-resolution anatomical images due to the high contrast that can be generated within an efficient total scan time. The time required for a redistribution of the energy from the RF excitation pulse to the surrounding medium or lattice is referred to as the T_1 time constant. Formally the T_1 time constant of a sample is the time required to re-establish 63% of the equilibrium longitudinal magnetization (M_z). Different tissue types and biological fluids, such as gray matter, white matter and CSF have different T_1 and T_2 time constants. These differences in relaxation times drive the contrast between tissue types. T_1-weighted images are important for anatomical neuroimaging. These images render the CSF and other fluid compartments dark (low signal intensity), while in contrast, brain parenchyma generates greater signals and hence

brighter pixel intensities in comparison to fluid cavities. A T_1 re-growth curve (Figure. 1-1.) can be generated to describe the return of the longitudinal component of the magnetization to equilibrium. Different biological mediums have different T_1 time constants and therefore relax to equilibrium at different rates. For the acquisition of T_1-weighted FLASH images, generally, an excitation pulse is repeated at a set interval of time called the repetition time (TR). The amount of recovery of equilibrium magnetization during the TR interval will depend on the tissue's T_1 time constant. A medium with a longer T_1 will recover less and therefore contribute signal less to the next excitation in comparison to a medium with a shorter T_1 relaxation time constant. Therefore, the medium with the shorter T_1 time constant will appear brighter in comparison to the medium with a longer T_1 time constant. A typical T_1 value for CSF is ~1900 ms whereas white matter is ~500ms at 1.5 Tesla.
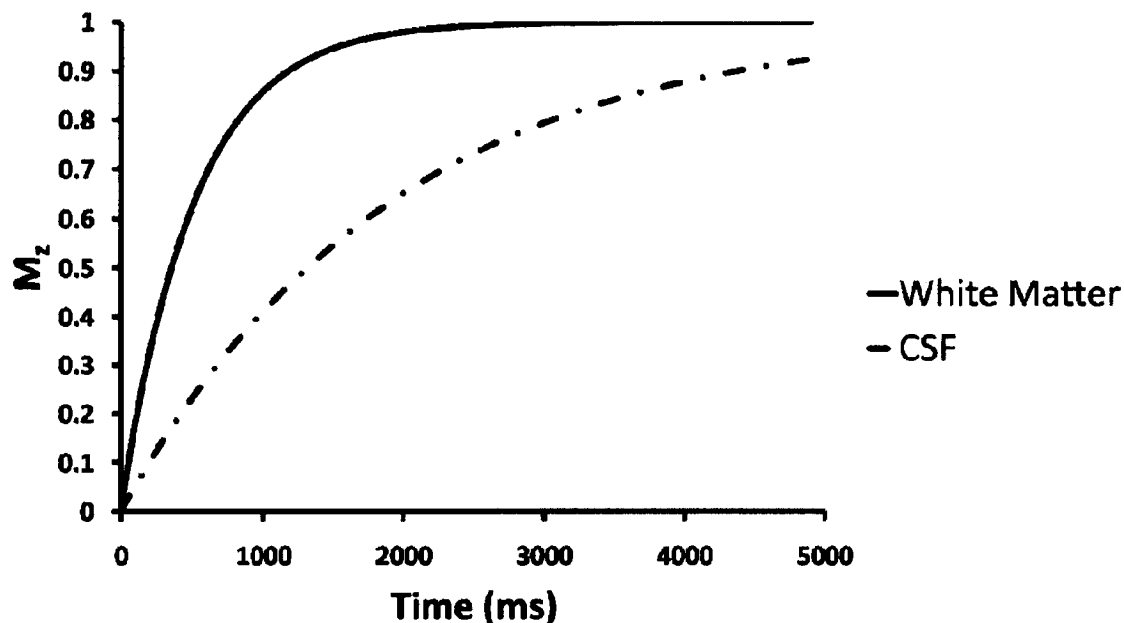
Figure 1-1. T_1 recovery curve of CSF and white matter. The longitudinal magnetization (M_z) recovery as a function of time after a 90° RF pulse saturates the spin system or alternatively excites all of the spins into the trasversal plane. Different tissues have different longitudinal recovery times depending on the T_1 time constant of the tissue. CSF has a longer recovery time than white matter and therefore will contribute less signal upon subsequent excitations in comparison to the signal from white matter.

Ultimately, the sharp contrast between CSF and white/grey matter parenchyma as a result of different T1 time constants between tissues renders a well defined ventricular boundary. Subsequently, precise volumes can be quantified by volumetric techniques. This provides a method of measuring brain structure and change *in vivo*. These structural measures can be used as markers of progression in persons with AD.

1.2.3 MRI BIOLOGICAL MARKERS FOR AD

A biomarker is as a biological or laboratory derived specimen linked to an underlying disease process that reflects the severity or state of the disease (Jagust. 2004). A surrogate marker can be defined as "a laboratory measurement or physical sign that is used in therapeutic trials as a substitute for a clinically meaningful endpoint that is a direct measure of how a patient feels, functions, or survives and is expected to predict the effect of the therapy" (Temple. 1999). According to Katz a biomarker is a *candidate* surrogate marker (Katz. 2004). Neuroimaging techniques may provide feasible biomarkers to measure AD progression. There are three salient roles a biomarker may have (Fox and Growdon. 2004). Specifically, a biomarker can be a measure of a disease trait or the likelihood of developing a trait; a marker could also measure disease state, for example the size of the lateral ventricles in AD (Fox and Growdon. 2004). Finally, a marker could be a measure of rate or the progression of a disease from serial measurements (Fox and Growdon. 2004). The most extensive biomarker research experience in AD derives from structural MRI (Schuff and Zhu. 2007). Kentarci *et al.* have defined a valid candidate MRI-based biomarker of AD as a measure that is sensitive to suspected pathologic changes in persons with clinical AD, sensitive to preclinical and prodromal AD, capable of predicting future progression to AD, reflecting the pathologic disease stage across the entire severity spectrum, serial measurements that correlate with clinical disease progression, and a marker that correlates with disease progression during therapeutic trials (Kantarci and Jack. 2004). Although it is likely that most biomarkers will not completely fulfill all these criteria. To further validate an MRI derived biomarker for AD, an appropriate sample of subjects must be selected. This would include selecting people with an average age around 80 (Jagust. 2004). Atrophy and increased protein marker levels observed in AD subjects are also associated with aging (Chung, et al. 2006, Sjogren, et al. 2001). Most studies in AD recruit participants from tertiary memory clinics. Therefore, these samples do not represent the general population. Community samples, although less convenient to recruit participants, may provide an alternative sample. Moreover, education has a putative effect on cognition and may markedly impact the validity of neuroimaging AD studies (Sanchez, et al. 2002).

In addition to constructing a valid measurement tool, such techniques under investigation should provide adequate test-retest reproducibility (precision). A sufficiently powered test-retest study should be conducted prior to analyzing MRI data. Such a study may be designed, which uses two independent blinded raters to evaluate the same sample and who perform these measurements at different time points (Walter, et al. 1998). An intraclass correlation coefficient (ICC) can be computed to assess consistency over time and between raters (Walter, et al. 1998). Automated tools characteristically yield higher consistency between raters and within raters in comparison to manual planimetric methods by an expert operator (Dade, et al. 2004). However, automated and semi-automated methods such as region-growing tools may be susceptible to measurement error based on image artefacts, inhomogeneities and partial voluming effects. In considering the potential utility of a measurement tool, a repeatability analysis of the tool is warranted. This is a measure of the intrinsic measurement stability of a technique. A suitable design would involve scanning a subset of subjects several times within a short interval. An assumption of this design is that there is no change over this short period due to disease processes. Therefore, any differences in the measured volumes between MR images would be likely attributable to measurement instability – provided intra-rater agreement is sufficiently high.

1.2.4 INTRODUCTION TO MRI CEREBRAL VENTRICULAR VOLUMETRY TECHNIQUES

The first measurements of the lateral ventricles were derived from CT (Huckman, et al. 1975) and employed linear measurement methods (Gado, et al. 1983). These tools were based on diameters of ventricular sub-volumes and allowed semi-quantitative measurement (Gado, et al. 1983). DeLeon and others first investigated quantitative ventricular measurement using CT (de Leon, et al. 1989a). These techniques required extensive manual tracing that was susceptible to operator error, and the *peri*-ventricular interface was poorly delineated and susceptible to partial-voluming errors (de Leon, et al. 1989b). MRI replaced CT as the *de facto* gold standard modality for neuroimaging studies in AD (Lehericy, et al. 2007). MRI provided comparable spatial-resolution to CT,

excellent brain tissue contrast (Rapoport. 1997), supported better imaging of the MTL in comparison to CT (Although advances in CT technology have improved spatial resolution to levels that are equivalent to clinical MRI scan resolution) (Rapoport. 1997), was amenable to more robust and rapid segmentation techniques and did not expose the subject to ionizing radiation (Lehericy, et al. 2007). Over the next decade, volumetric slice-by-slice tracing methods, using graphical tools, were used extensively to measure ventricular volumes (de Leon, et al. 1989c, DeCarli, et al. 1992). However, these planimetric methods constrain sample sizes and are labour-intensive (Dade, et al. 2004). The advent of enhanced processing power and more sophisticated algorithms, dramatically improved techniques for ventricular volumetry. Thereto, semi-automatic methods to quantify the ventricles developed (Giesel, et al. 2006, Schott, et al. 2005). These methods provided a means to address the problems arising from the intrinsic complexity of image data due to noise and inhomogeneous pixel intensity distribution within the ventricles. For instance, choroid tissue within the ventricles can lead to spurious segmentation results. Moreover, these technologies allow the human expert to exploit images in an objective manner. Several semi-automated and fully automated approaches exist including, region-growing algorithms (Dellepiane. 1997), shape modeling (Ferrarini, et al. 2006), voxel-wise techniques (i.e. compares signal intensity voxel-by-voxel between two groups of subjects to determine gray matter concentration) (Jack, et al. 2008) and tensor based morphometric approaches (Rose, et al. 2008). Semi-automated region segmentation methods allow for minimal user-friendly quality control whilst are powerful and minimally interactive.

1.2.5 BRAIN VENTRICLE QUANTIFICATION REGION-GROWING ALGORITHM

For semi-automatic purposes, there are two prevailing approaches for region-segmentation. The first class, binary segmentation, evaluates for every voxel in an MR volume whether or not a given voxel belongs to an anatomical structure of interest based on a threshold value or function of intensity (Accomazzi, et al.). Gray-level segmentation is another useful method which provides a level of confidence for each voxel in the image, based on a function, to determine membership within a structure (Dellepiane.

1997). No *a priori* threshold is required in comparison to the binary technique (Accomazzi, et al.). Subsequently, a connectivity map is generated which assigns a level of confidence to each voxel in the image (Saha, et al. 2000). This will produce a number of solutions that depend on the minimal level of confidence chosen.

An attractive method for producing a gray level segmentation is a region-growing procedure based on fuzzy labelling. This method is particularly suitable for segmenting the cerebral lateral ventricles. Brain Ventricle Quantification (BVQ) (Cedara Software, Mississauga, Ontario) is a modified region-growing algorithm predicated on fuzzy labelling techniques for the purpose of segmenting the lateral ventricles (Accomazzi, et al.). There are two important features to this procedure which include the fuzzy labelling region-growing process and the selection of an optimal intensity threshold. The region-growing procedure is initiated by a trained operator placing seed points in the lateral ventricles, Figure 1-1. The fuzzy labelling procedure ascribes a value ranging from 0 to 1 to each voxel (Dellepiane. 1997). Such a value denotes the degree of membership in the volume identified by a reference seed point. The seed point is labelled as 1 with surrounding voxels containing constant or decreasing membership values. Membership values are generated for each connected voxel by a function of intensity and distance from the original user-placed seed point. For each voxel being evaluated, all paths between the voxel of interest and the seed point are considered by the algorithm. Each voxel along each path is evaluated individually based on both intensity and distance in relation to the seed point. The total of these differences for each voxel along each path is summed. The path with the minimum sum total is selected. Ultimately, this is the path with the shortest distance from the seed point and also contains the greatest number of voxels with similar intensity to the seed point. This value is then used to render a membership value to the voxel under investigation. On the basis of this region-growing procedure, a segmented three dimensional (3D) MRI may be interpreted as a 3D topological map of membership values, from which one can derive a set of ventricular volumes (Accomazzi, et al.). The highest membership values correspond to points that are most likely to belong to the ventricle.
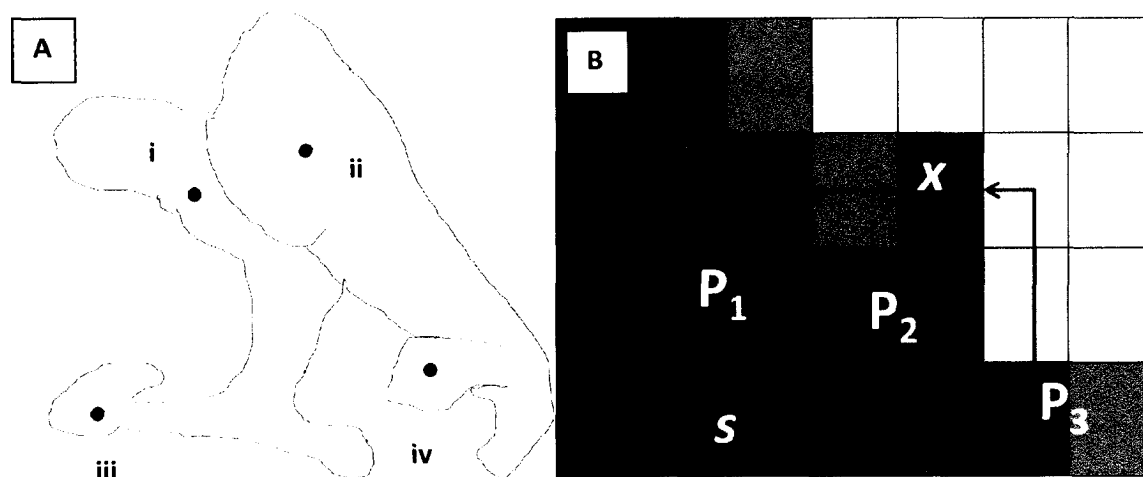
Figure 1-2. (a) the round markers represent typical seed point placements within the lateral ventricles i) the right anterior horn, ii) the left anterior horn, iii) the right temporal horn, iv) the left temporal horn. Fig 1-1 (b) illustrates the fuzzy labelling process: Three hypothetical paths have been selected for illustrative purposes: the label value for voxel x is determined by pathway 2 (P_2) since the sum of the differences in pixel intensities and distances from the seed point (s) is least for each voxel in P_2 in comparison to P_1 or P_3. A label would then be given to this voxel between 0 and 1. This label value is then subtracted from 1, generating a "connectivity value". A connectivity value close to 1 indicates a high level of confidence that the voxel x belongs to the same structure as the seed point.

The concept of an optimal threshold is also central to an accurate segmentation. The optimal threshold for a given segmentation is selected in a recursive fashion. The optimal threshold is selected by evaluating the volume of the region segmented as a function of the threshold intensity selected, Figure 1-2. First, the algorithm selects three initial intensities as threshold values based on previous knowledge of intensities of the ventricles. BVQ samples a threshold at a high intensity, a threshold at a low intensity and mid-intensity. The threshold is progressively updated until it reaches a point on the intensity volume curve where there is a dramatic increase in volume with a small change in threshold value, Figure 1-3. For small changes in threshold value, a small variation in the volume is typically realized. Alternatively, when there is a small increase in the variation of the threshold value and a large increase in the volume, the algorithm has

likely included background structures, Figure 1-3. The more conservative the threshold value, the less ventricular volume will be included. Ultimately, the algorithm will grow in 3-D until it reaches the *peri*-ventricular boarder and renders a volume based on the optimal threshold for a given image. Any extraneous anatomy such as the third ventricle communicating through the foramen of Monroe, the fourth ventricle, the ambient cistern or the cerebral aqueduct can be precisely excised by an operator via a suite of proprietary tools developed by, Cedara Software.
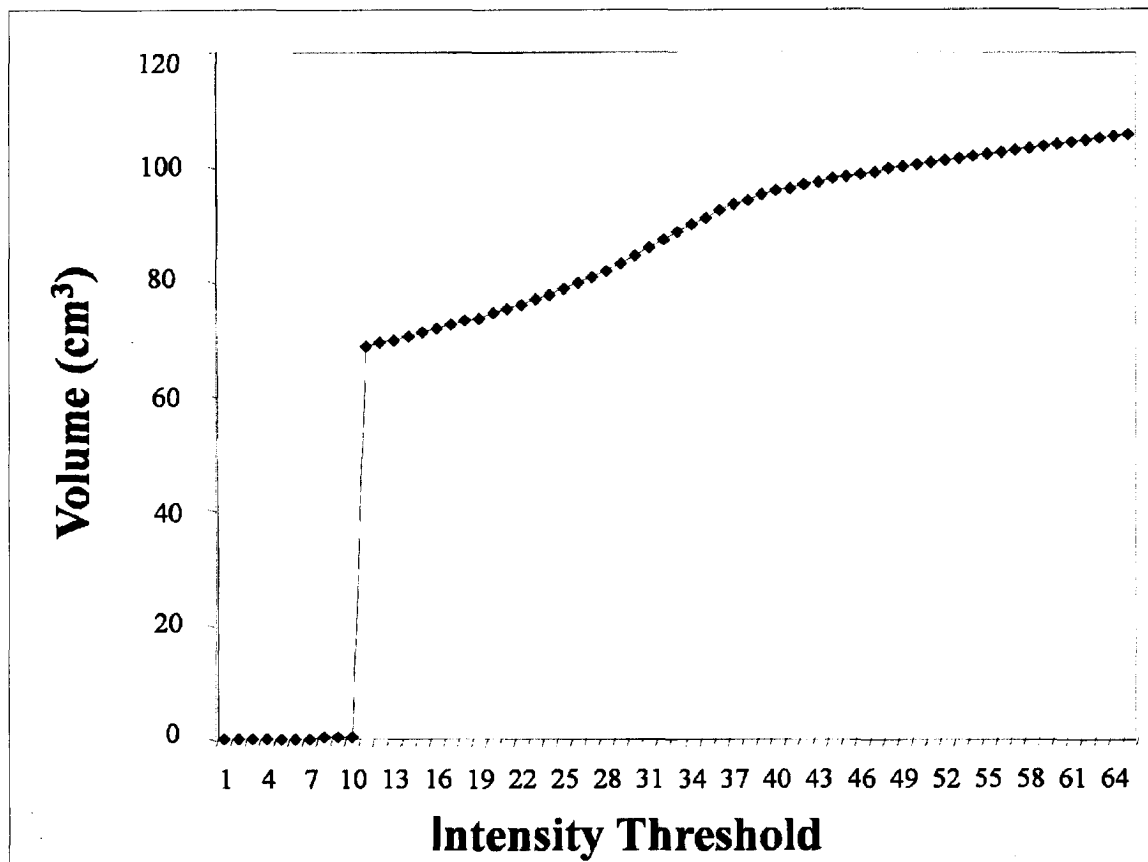
Figure 1-3. Lateral ventricular volume-intensity threshold plot. From the plot of ventricular volume and selected intensity threshold, an optimal intensity threshold can be selected using a binary recursive procedure. The algorithm selects two values then recursivly finds the optimal threshold just before there is a sharp increase in volume for a small variation in intensity. Alternatively, this is the point where the first derivative of the inensity volume curve becomes discontinuous. Image courtesy of Vittorio Accomazzi, Cedara Software.
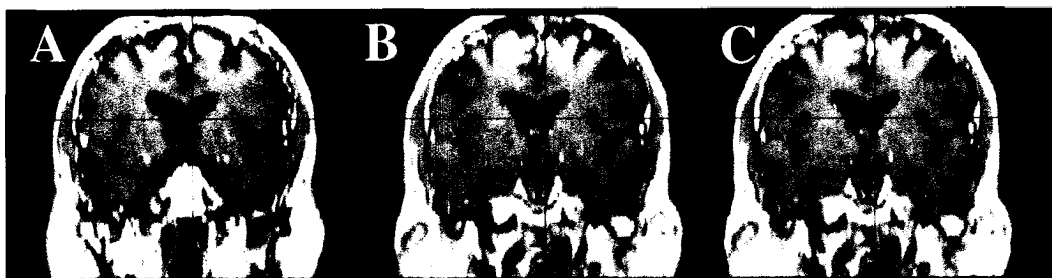
Figure 1-4. Brain Ventricle Quantification software region-growing optimal threshold selection. Coronal MRI (a) demonstrates a threshold which underestimates the ventricular volume, image (b) demonstrates an optimal threshold for ventricular segmentation and image (c) overestimates the ventricular volume, which includes extraneous CSF structures. Image courtesy of Vittorio Accomazzi, Cedara Software.

The intrinsic complexity of the ventricles provides a challenge for gray-level segmentation algorithms. The ventricles are heterogeneous CSF cavities that narrow, particularly around the MTL (temporal horn) and occipital lobe (posterior cornu) in healthy persons. For these reasons, placing a seed point in each of the ventricular bodies is not sufficient for an accurate segmentation. The distance function in the region-growing procedure also constrains the volume of CSF segmented. Including two additional seed points in the temporal horns provides a solution for segmenting temporal horn structures, even when they do not communicate with the ventricular body. Figure 1-5 demonstrates a ventricle without temporal horn seed placement and with two additional seed points.
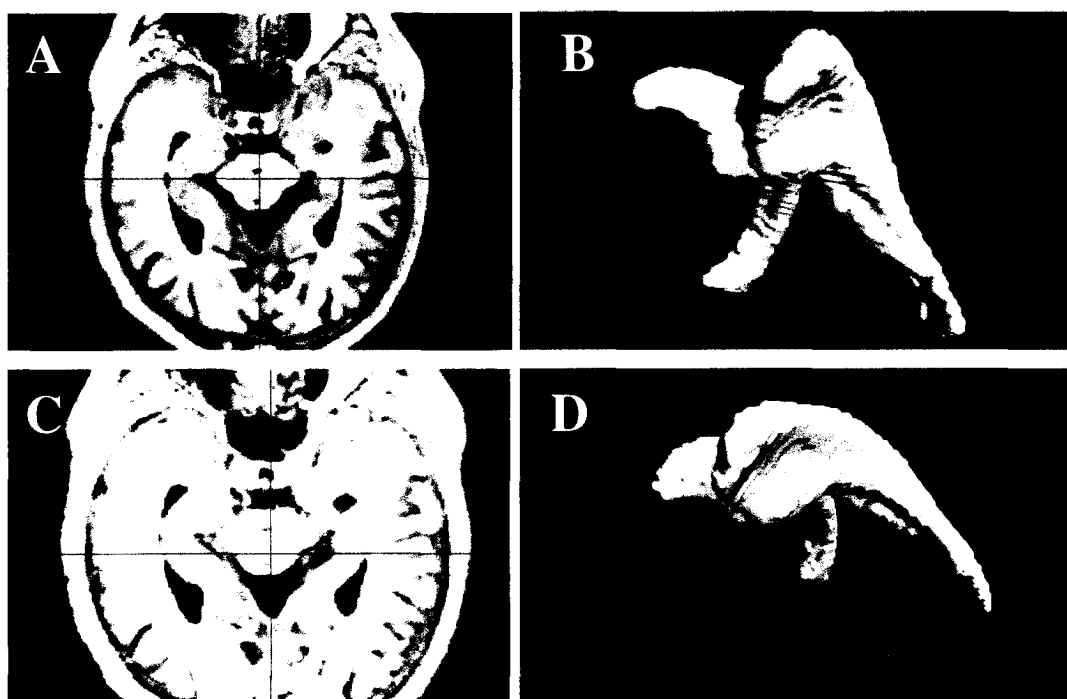
Figure 1-5. Seed point placement within the lateral ventricles. Axial (A), 3D rendered (B), T_1-weighted MRI images of one subject with the pixels assigned to the lateral ventricles by the Brain Ventricle Quantification software colored in red. In images (A) and (B) only two seed points were placed in the ventricular bodies, and the volume was underestimated. Axial (C), 3D rendered (D), T_1-weighted MRI of the same subject as (A) and (B) with two additional seed points placed in the anterior temporal horns.

The temporal horns of the lateral ventricles are anatomically situated adjacent to the dentate gyrus of the hippocampus, the fornix, and tail of the caudate nuclei. Parahippocampal regions notably atrophy in early AD and MCI. Temporal horn volume provides a precise way to indirectly quantify MTL pathologic change. The ventricles conform to a concave surface at the posterior thalamic border, which is known as the bilateral trigones. The trigones provide an eloquent and automatic method for segmenting the temporal horns. By taking the tangent point of the right and left trigones a plane can be computed orthogonal to the temporal horns. This delineates the posterior border of the temporal horns. Moreover, this plane approximately bisects the posterior tip of the inferior colliculus which is an anatomical landmark previously described in a manually-

intensive method of temporal horn segmentation (Giesel, et al. 2006). Figure 1-5 demonstrates the plane created by the BVQ algorithm.
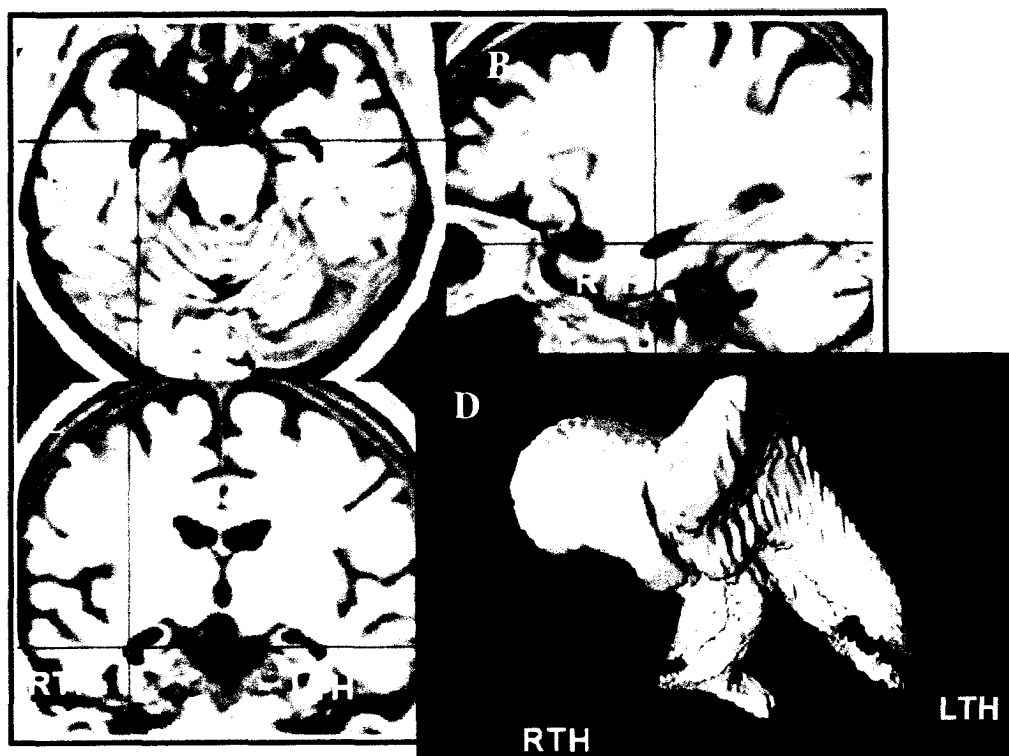
Figure 1-6. Temporal horns of the lateral ventricle. Axial (A), sagittal (B), and coronal (C) T_1-weighted MRI images of one subject with the pixels assigned to the lateral ventricles by the Brain Ventricle Quantification software colored in red. The orthogonal lines intersect the right temporal horn of the right lateral ventricle. A three-dimensional rendered view of the ventricle from this subject (D) with the right temporal horn (RTH) and left temporal horn (LTH) depicted in green and red respectively.

The intrinsic precision of BVQ was measured using a repeatability study. Specifically, 10 healthy controls were scanned on a 4.0 Tesla Varian, Palo Alto, CA, USA, MRI scanner using a T_1-weighted protocol (in-plane matrix size = 256 x 256, slice thickness = 2.5 mm, TI = 500 ms, TR = 510 ms, TE = 5.3 ms). Ethics approval was obtained from the University of Western Ontario office of research ethics (Appendix). Each subject underwent three sequential MR scans with re-placement of the head before each scan.

The three scans for each subject were then measured by the same operator (S.N.) to evaluate the repeatability of the ventricular volume measured by BVQ. The operator was blind to subject and scan order. Reproducibility was calculated using an ICC. The ICC was 0.97, 95% confidence interval = 0.94-0.99. The precision of BVQ is excellent. This high value reflects the high reproducibility of this technique. The scans were acquired in sequential order on healthy controls; therefore, changes in brain volume have no appreciable effect on ventricular change between scans. Any change can be attributed to the operator, image or BVQ. However, because intrarater reliability was determined to be high (chapter 2) and the images were acquired on the same magnet during the same visit, it is likely that most measurement instability could be attributed to BVQ.

1.2.6 STUDIES OF VENTRICULAR VOLUMETRY IN MCI AND AD

Matthew Baillie in the eighteenth century first remarked on cerebral atrophy in the demented individual post-mortem and observed enlarged ventricles in persons with dementia (Berchtold and Cotman. 1998). Although Baillie astutely noted differences in the brains of persons with dementia, ventricular enlargement was unrecognized as a correlate of cerebral atrophy for centuries; however, by the late nineteenth century, cerebral atrophy was well documented in the *post-mortem* brains of persons with dementia (Berchtold and Cotman. 1998). The clinical inception of CT neuroimaging provided a method to characterize *in-vivo* brain changes. Huckman and colleagues in 1975 were the first to report *in vivo* CT derived ventricular differences in persons with dementia (Huckman, et al. 1975). Gado *et al.* in 1983 reported the first longitudinal study demonstrating ventricular enlargement in persons with dementia of the Alzheimer's type after one year follow-up (Gado, et al. 1983). These studies employed linear measurement techniques relying on scaled tracings of the width of the third ventricle, bifrontal span of the lateral ventricle in the coronal plane, the width of the bodies of the lateral ventricles and the caudate span visualized in the coronal plane (Gado, et al. 1983). Region of interest (ROI) volumetric methods supplanted linear techniques as the *de facto* gold standard. ROI methods provided superior sensitivity to capture volumes of a complex shape for example the lateral ventricle (Luxenberg, et al. 1987). More sophisticated

quantitative methods were used by DeLeon et al. in 1989 (de Leon, et al. 1989a). However, spatial resolution remained poor with CT techniques with slice thicknesses of approximately 10mm (Shear, et al. 1995). Neurospychological correlates of ventricular expansion were extensively described by DeCarli et al. in 1992 (DeCarli, et al. 1992). As MRI replaced CT as the principle neuroimaging research modality in AD with its superior tissue contrast and non-ionizing radiation, greater spatial resolution was realized and more accurate quantitative methods evolved. Scientific progress in the field of structural imaging, including the use of image co-registration, and semi-automatic algorithms, have dramatically improved the precision and accuracy with which small volume changes can be measured over short intervals in normal aging, MCI (Carmichael, et al. 2007) and AD (Jack, et al. 2004a). Silbert *et al.* first demonstrated the association between ventricular volume and histopathalogically confirmed AD at post-mortem (Silbert, et al. 2003). Jack *et al.* later demonstrated that ventricular enlargement provided superior sensitivity to AD brain changes in comparison to whole brain change, hippocmapal shrinkage and entorhinal cortex atrophy (Jack, et al. 2004a). One explanation to support these results is the sharp contrast realized between the ventricles and *peri*-ventricular brain parenchyma allows for accurate segmentation in comparison to the borders of other MTL structures. Longitudinal studies of ventricular change over a decade support the notion that persons with incipient AD demonstrate an accelerated signature of ventricular expansion prior to clinical diagnosis in comparison to healthy controls (Carlson, et al. 2008). However, cross-sectional studies of ventricular volumes repeatedly show marked overlap between NEC, MCI and AD group-wise comparisons (Carmichael, et al. 2007, Schott, et al. 2005, Wang, et al. 2002). This heterogeneity has obviated the need to measure the rate of ventricular change and has also motivated the development of quantitative sub-volume technologies and temporal horn semi-quantitative scales (Giesel, et al. 2006). In particular, Ferrarni *et al.* described specific regions of ventricular enlargement with the greatest signal emanating from the temporal horns and ventricular trigones (Ferrarini, et al. 2006). These structures are adjacent to the lateral border of the hippocampal formation and deep white matter structures of the caudate nuclei, fornix and thalamus. Sub-volume changes may provide a focal and more sensitive measure of MTL structural change (Ferrarini, et al. 2008).

1.2.7 MRI, THE APOLIPOPROTEIN ε4 ALLELE AND AD

ApoE ε4 has been unequivocally identified as a susceptibility gene for late onset AD (Bizzarro, et al. 2005). Apolipoprotein E is a polymorphic gene with three principle isoforms in humans: ε2, ε3 and ε4 (Corder, et al. 1993). Extensive genetic studies suggest that persons with an ε4 allele have a 20 fold greater risk of developing AD (Bu. 2009). In a Canadian study the allelic frequencies were 7.8% (ε2), 77% (ε3) and 15.2% (ε4) (Swartz, et al. 1999). The prevalence of the ε4 allele, however, dramatically increases in an AD sample (Corder, et al. 1993). Apolipoprotein E is a critical modulator of cholesterol and phospholipid transport between cells (Mahley. 1988). Specifically, the primary function of ApoE in the brain is to transport cholesterol from astrocytes to neurons (Mahley. 1988). Its role in the pathogenesis of AD is still unclear and may involve several mechanisms. Cholesterol is required for synaptic viability and neuronal function, and evidence suggests the ε4 isoform is less efficient at transporting cholesterol in the brain in comparison to other ApoE isoforms (Bu. 2009). ApoE has been demonstrated to bind to Aβ and facilitate Aβ clearance into the plasma through ApoE receptors at the blood brain barrier (Swartz, et al. 1999). The ε4 isoform is less efficient at clearing Aβ in comparison to the ε2 and ε3 variants (Bu. 2009). The ε4 isoform has also been implicated in aberrant Aβ processing (Ye, et al. 2005). Several lines of evidence suggest that ApoE ε4 may also contribute to impaired neuronal repair mechanisms following brain injury and oxidative damage (Bu. 2009). Clinicopathalogical relationships between ApoE genotypes and AD have motivated the exploration of neuroimaging-genotype association studies (Basso, et al. 2006, Chen, et al. 2007, den Heijer, et al. 2002, Moffat, et al. 2000). Several imaging studies have demonstrated an association between the ApoE ε4 allele and atrophy of the MTL (Bigler, et al. 2000, Moffat, et al. 2000, Visser, et al. 2005) and whole brain atrophy (Chen, et al. 2007, Swartz, et al. 1999, Wahlund, et al. 1999). However, neuroimaging and ε4 studies in AD vary in methodological approach and most studies derive results from small samples. A recent qualitative review of ApoE-neuroimaging studies in MCI and AD suggests that ε4 has an effect in prodromal, preclinical and mild AD (Cherbuin, et al. 2007). The majority

of endophenotypic studies of the ApoE genotype examine hippocampal and whole brain volume measurements (Cherbuin, et al. 2007). Few studies report associations between ventricular volume and the ApoE genotype. Larger and well-controlled studies are warranted to detect brain structure differences between ApoE genotypes in the healthy elderly, persons with MCI and AD, and to elucidate the role of ApoE ε4 in the progression of AD.

1.2.8 POWER ANALYSIS FOR CLINICAL TRIALS IN MCI AND AD

Several purported disease modifying therapies are currently under investigation (U.S. National Institute of Health. May 2009). Current endpoints are predicated on neurobehavioural and cognitive tests (Petersen, et al. 2005, Wilcock, et al. 2000). These tests can only report symptomatic therapeutic benefit and can not substantiate biological efficacy. Moreover, to detect treatment effects in RCTs large samples are required (>500 persons) (Petersen, et al. 2005, Wilcock, et al. 2000). Candidate biomarkers such as lateral ventricular volumes derived from MRI may provide a means to indirectly demonstrate a change in brain-parenchymal loss from the natural history of the disease. Moreover, hypothetical power calculations computed from observational samples, have demonstrated fewer persons are required to detect treatment differences in a RCT when biological markers are used as endpoints (Ridha, et al. 2008). A power analysis such as equation 1-1 (Fox, et al. 2000) provides a method to directly compare the utility of biomarkers when the same sample of subjects is evaluated.

$$\text{Sample size} = (u + v)^2(\sigma_1^2 + \sigma_2^2)/ (\mu_1 - \mu_2)^2 \qquad [1\text{-}1]$$

Where $u=1.28$ to provide 90% power and $v =1.96$ to test at the 5% level; μ and σ are the mean and standard deviations of the rates of atrophy in the treatment and placebo groups (assumes $\mu1 \sim \mu2$). Ideally an effective candidate biomarker would yield small sample sizes, usually less than 100 subjects per arm of a study (Ridha, et al. 2008), when serial measurements are performed after 1 year follow-up. This is the approach the biostatistical core for the ADNI is employing to compare biomarkers across modalities and

measurement techniques (complete listing available at www.loni.ucla.edu\ADNI\Collaboration\ADNI_Citation.shtml. 2007). However, other factors may contribute to the viability of a candidate biomarker including how robust the marker is to image artefacts and inhomogeneities. Although a technique may provide sufficient sensitivity to detect treatment effects it may only work on high-quality images with superior signal-to-noise ratios.

1.2.9 THE ALZHEIMER DISEASE NEUROIMAGING INITIATIVE

A major focus of clinical studies in AD is evaluation of the predictive value of AD biomarkers and longitudinal biomarker changes in persons with MCI who progress to AD (Dubois, et al. 2007). To this end, the longitudinal AD study the Alzheimer Disease Neuroimaging Initiative was designed to refine and validate the biomarker methods that have shown promise for early detection of AD (Shaw. 2008). The ADNI includes 3 cohorts of study subjects: normal elderly controls (NEC) (N=200), subjects with MCI (N=400) and persons with AD (N=200) to be observed over three years. This study is a multicentre consortium study comprised of 58 study sites in Canada and the US. It is funded by the National Institutes of Health, industry and foundations. Biological samples including DNA, serum, plasma, urine, CSF, MRI, PET, Fludeoxyglucose positron emission tomography (FDG-PET), PIB PET are collected and banked by the ADNI core labs. In addition, neuropsychological, neurobehavioral, clinical, patient histories are recorded and processed centrally in ADNI. An ADNI MRI core (Jack, et al. 2008) and PET core (Langbaum, et al. 2009) perform all quality control evaluations and perform ADNI specified post-processing procedures. These data are then available for download from www.ADNI_LONI.com. There are three major goals of ADNI. The first goals is to develop improved methods that will lead to uniform standards for acquiring longitudinal, multicentre MRI and PET data on patients with AD, MCI and NEC. The second goal is to create a generally accessible data repository that describes longitudinal changes in brain structure and metabolism while acquiring clinical, cognitive and biomarker data for validation of imaging surrogates. The final goal is to determine those methods that provide maximum power to determine treatment effects in trials involving these patient groups. It is expected that ADNI will substantiate candidate biomarkers measuring the

natural course of brain changes, which occur during the transition from normal aging to MCI to AD that can be used to improve the power of MCI and AD clinical trials and obtain information about the relationship between neuroimaging, serum, and CSF.

Core ADNI funded investigators and specific ADNI users have been invited to contribute their data to the ADNI database. For this purpose, our group as of January 2009 has contributed ~3000 ventricular volume measurements to the ADNI database. These data are directly compared with other contributed biomarkers. A direct comparison using a power analysis by the ADNI statistical core headed by Dr. Laurel Becket will be performed to determine which biomarkers provide the greatest sensitivity for a hypothetical reduction in the rate of change in biomarkers over one year.

1.2.10 THE ADNI MRI-CORE METHODS

The primary goal of the ADNI MRI-core is to standardize a structural MRI pulse sequence across MR vendors and platforms (Jack, et al. 2008). The Magnetization Prepared Rapid Acquisition Gradient Echo (MP-RAGE) sequence was selected after a mini randomized trial (Jack, et al. 2008). The MP-RAGE sequence has superior gray matter / white matter contrast to noise ratio, superior performance in some applications requiring cortical segmentation, and imaging times that were less than 10 minutes across vendor platforms in addition to phantom scans (Jack, et al. 2008). The entire scanning visit requires approximately 30 minutes per participant. Participants receive two high resolution 3D T_1 weighted back to back scans in addition to an axial proton density/T_2 dual contrast Fast Spin Echo/ True Spin Echo. This optimizes the scientific utility and minimizes the research burden on the participants. The qualities of all scans are then evaluated at the Mayo clinic using a four-point scale: none, mild, moderate, and severe based on artefacts, tissue contrast, inhomegenities and signal to noise ratio (Jack, et al. 2008). T1-weighted scans are scaled to a phantom image acquired as part of each patient visit. This facilitates retrospective rescaling of human images to correct for drift or discontinuities in gradient calibration. These phantom acquisitions also provide a means to evaluate scanner performance over time (Jack, et al. 2008).

1.3 OBJECTIVES

In summary, brain changes over short intervals, derived from multi-centre data, have not been reported in persons with MCI or AD. Although there have been several studies evaluating brain changes using single-centre MRI data, the majority of studies are cross-sectional and do not demonstrate changes over short intervals of less than 1 year. By refining the novel region-growing algorithm BVQ (Cedara Software), which is both a rapid and reproducible technology, to segment the lateral cerebral ventricles, a clear characterization of global brain change in healthy aging, MCI and AD may be achieved using multicentre data. The objectives of this thesis were as follows:

[I]   To refine the semi-automatic segmentation tool Brain Ventricles Quantification (BVQ)

[II]   To test the measurement stability in healthy controls at 4.0 Tesla. We hypothesized that ventricular volumes would be similar across multiple scans. An ICC was used to test this hypothesis.

[III]   To evaluate the reliability of the BVQ algorithm. We expected a high level of agreement for ventricular measurements between operators and within operators. An intraclass correlation coefficient and interclass correlation coefficient was used to evaluate reliability.

[IV]   To compare group-wise differences of ventricular volume and ventricular enlargement between AD, MCI and NEC subjects from a multi-centre study. We expected baseline volumes and ventricular enlargement to be greater in AD in comparison to MCI and NEC. We expected subjects with MCI to have greater volumes and ventricular expansion than NEC. Group-wise omnibus F-tests were used to test these hypotheses.

[V]   To determine if ventricular enlargement can differentiate subjects progressing from MCI to AD and those persons with MCI that remain stable at baseline. We expected MCI progressors to have a greater rate of ventricular enlargement than people with MCI remaining stable. A t-test was employed to evaluate differences between MCI groups.

[VI]   To investigate the relationship between ApoE genotype and structural brain changes in subjects with NEC, MCI and AD. We expected subjects with an ApoE ε4 genotype to demonstrate a greater rate of ventricular enlargement in comparison to persons without an ε4 allele. An ANCOVA was used to evaluate group-wise differences.

[VII]   To determine the number of subjects necessary to detect a meaningful change from the natural history of ventricular enlargement with respect to genotype. We expected ventricular measures to derive smaller sample sizes in comparison to cognitive measures. A sample size calculation was used to test this hypothesis.

[VIII]   To correlate ventricular change with neuropsychological test scores after a short six-month interval from baseline. We expected ventricular change to correlate with cognitive decline. Pearson correlations were used to evaluate the association between cognitive and ventricular measurements in each group.

1.4 REFERENCES

Accomazzi V, Lazarowich R, Barlow CJ, Davey B. Image region segmentation system and method.

Alexopoulos P, Grimmer T, Perneczky R, Domes G, Kurz A. Do all patients with mild cognitive impairment progress to dementia?. J Am Geriatr Soc 2006; 54: 1008-10.

Alzheimer's Disease Neuroimaging Initiative www.loni.ucla.edu\ADNI\Collaboration\ADNI_Citation.shtml. Alzheimer's disease neuroimaging initiative (ADNI). 2007; 2007.

Alzheimer's Society of Canada. Alzheimer's disease fact sheet. http://www.alzheimer.ca/english/media/adfacts2009.htm. January 2009; May 2009: 1.

American Psychiatric Association, American Psychiatric Association. Diagnostic and statistical manual of mental disorders : DSM-IV-TR. Washington, DC: American Psychiatric Association; 2000.

Barron SA, Jacobs L, Kinkel WR. Changes in size of normal lateral ventricles during aging determined by computerized tomography. Neurology 1976; 26: 1011-3.

Basso M, Gelernter J, Yang J, MacAvoy MG, Varma P, Bronen RA, et al. Apolipoprotein E epsilon4 is associated with atrophy of the amygdala in Alzheimer's disease. Neurobiol Aging 2006; 27: 1416-24.

Berchtold NC, Cotman CW. Evolution in the conceptualization of dementia and Alzheimer's disease: Greco-roman period to the 1960s. Neurobiol Aging 1998; 19: 173-89.

Bigler ED, Lowry CM, Anderson CV, Johnson SC, Terry J, Steed M. Dementia, quantitative neuroimaging, and apolipoprotein E genotype. Ajnr: American Journal of Neuroradiology 2000; 21: 1857-68.

Bizzarro A, Marra C, Acciarri A, Valenza A, Tiziano FD, Brahe C, et al. Apolipoprotein E epsilon4 allele differentiates the clinical response to donepezil in Alzheimer's disease. Dementia & Geriatric Cognitive Disorders 2005; 20: 254-61.

Braak H, Braak E. Morphological criteria for the recognition of Alzheimer's disease and the distribution pattern of cortical changes related to this disorder. Neurobiol Aging 1994; 15: 355,6; 379-80.

Bradley KM, Bydder GM, Budge MM, Hajnal JV, White SJ, Ripley BD, et al. Serial brain MRI at 3-6 month intervals as a surrogate marker for Alzheimer's disease. Br J Radiol 2002; 75: 506-13.

Bu G. Apolipoprotein E and its receptors in Alzheimer's disease: Pathways, pathogenesis and therapy. Nature Reviews Neuroscience 2009; 10: 333-44.

Carlson NE, Moore MM, Dame A, Howieson D, Silbert LC, Quinn JF, et al. Trajectories of brain loss in aging and the development of cognitive impairment. Neurology 2008; 70: 828-33.

Carmichael OT, Kuller LH, Lopez OL, Thompson PM, Dutton RA, Lu A, et al. Ventricular volume and dementia progression in the cardiovascular health study. Neurobiol Aging 2007; 28: 389-97.

Chen K, Reiman EM, Alexander GE, Caselli RJ, Gerkin R, Bandy D, et al. Correlations between apolipoprotein E epsilon4 gene dose and whole brain atrophy rates. Am J Psychiatry 2007; 164: 916-21.

Cherbuin N, Leach LS, Christensen H, Anstey KJ. Neuroimaging and APOE genotype: A systematic qualitative review. Dement Geriatr Cogn Disord 2007; 24: 348-62.

Chung SC, Tack GR, Yi JH, Lee B, Choi MH, Lee BY, et al. Effects of gender, age, and body parameters on the ventricular volume of korean people. Neurosci Lett 2006; 395: 155-8.

Corder EH, Saunders AM, Strittmatter WJ, Schmechel DE, Gaskell PC, Small GW, et al. Gene dose of apolipoprotein E type 4 allele and the risk of Alzheimer's disease in late onset families. Science 1993; 261: 921-3.

Dade LA, Gao FQ, Kovacevic N, Roy P, Rockel C, O'Toole CM, et al. Semiautomatic brain region extraction: A method of parcellating brain regions from structural magnetic resonance images. Neuroimage 2004; 22: 1492-502.

de Leon MJ, George AE, Reisberg B, Ferris SH, Kluger A, Stylopoulos LA, et al. Alzheimer's disease: Longitudinal CT studies of ventricular change. AJR.American Journal of Roentgenology 1989a; 152: 1257-62.

de Leon MJ, George AE, Reisberg B, Ferris SH, Kluger A, Stylopoulos LA, et al. Alzheimer's disease: Longitudinal CT studies of ventricular change. AJR.American Journal of Roentgenology 1989b; 152: 1257-62.

de Leon MJ, George AE, Reisberg B, Ferris SH, Kluger A, Stylopoulos LA, et al. Alzheimer's disease: Longitudinal CT studies of ventricular change. AJR.American Journal of Roentgenology 1989c; 152: 1257-62.

DeCarli C, Haxby JV, Gillette JA, Teichberg D, Rapoport SI, Schapiro MB. Longitudinal changes in lateral ventricular volume in patients with dementia of the Alzheimer type. Neurology 1992; 42: 2029-36.

Dellepiane S. The active role of 2-D and 3-D images: Semi-automatic segmentation. In: Roux C, Coatrieux JL, editors. Contemporary Perspectives in Three-Dimensional Biomedical Imaging. Washington D.C.: IOS Press; 1997. p. 165-81.

den Heijer T, Oudkerk M, Launer LJ, van Duijn CM, Hofman A, Breteler MM. Hippocampal, amygdalar, and global brain atrophy in different apolipoprotein E genotypes. Neurology 2002; 59: 746-8.

Devanand DP, Pradhaban G, Liu X, Khandji A, De Santi S, Segal S, et al. Hippocampal and entorhinal atrophy in mild cognitive impairment: Prediction of Alzheimer disease. Neurology 2007; 68: 828-36.

Dubois B, Feldman HH, Jacova C, Dekosky ST, Barberger-Gateau P, Cummings J, et al. Research criteria for the diagnosis of Alzheimer's disease: Revising the NINCDS-ADRDA criteria.[see comment]. Lancet Neurology 2007; 6: 734-46.

Ferrarini L, Palm WM, Olofsen H, van Buchem MA, Reiber JH, Admiraal-Behloul F. Shape differences of the brain ventricles in Alzheimer's disease. Neuroimage 2006; 32: 1060-9.

Ferrarini L, Palm WM, Olofsen H, van der Landen R, Jan Blauw G, Westendorp RG, et al. MMSE scores correlate with local ventricular enlargement in the spectrum from cognitively normal to Alzheimer disease. Neuroimage 2008; 39: 1832-8.

Fjell AM, Walhovd KB, Amlien I, Bjornerud A, Reinvang I, Gjerstad L, et al. Morphometric changes in the episodic memory network and tau pathologic

features correlate with memory performance in patients with mild cognitive impairment. Ajnr: American Journal of Neuroradiology 2008; 29: 1183-9.

Fleisher AS, Sun S, Taylor C, Ward CP, Gamst AC, Petersen RC, et al. *Volumetric MRI vs clinical predictors of Alzheimer disease in mild cognitive impairment. Neurology 2008; 70: 191-9.*

Fox N, Growdon JH. *Biomarkers and surrogates. NeuroRx 2004; 1: 181.*

Fox NC, Cousens S, Scahill R, Harvey RJ, Rossor MN. *Using serial registered brain magnetic resonance imaging to measure disease progression in Alzheimer disease: Power calculations and estimates of sample size to detect treatment effects. Arch Neurol 2000; 57: 339-44.*

Gado M, Hughes CP, Danziger W, Chi D. *Aging, dementia, and brain atrophy: A longitudinal computed tomographic study. Ajnr: American Journal of Neuroradiology 1983; 4: 699-702.*

Giesel FL, Hahn HK, Thomann PA, Widjaja E, Wignall E, von Tengg-Kobligk H, et al. *Temporal horn index and volume of medial temporal lobe atrophy using a new semiautomated method for rapid and precise assessment. AJNR Am J Neuroradiol 2006; 27: 1454-8.*

Glenner GG, Wong CW. *Alzheimer's disease: Initial report of the purification and characterization of a novel cerebrovascular amyloid protein. Biochemical & Biophysical Research Communications 1984; 120: 885-90.*

Graeber MB, Kosel S, Egensperger R, Banati RB, Muller U, Bise K, et al. *Rediscovery of the case described by alois Alzheimer in 1911: Historical, histological and molecular genetic analysis. Neurogenetics 1997; 1: 73-80.*

Grundke-Iqbal I, Iqbal K, Quinlan M, Tung YC, Zaidi MS, Wisniewski HM. *Microtubule-associated protein tau. A component of Alzheimer paired helical filaments. J Biol Chem 1986; 261: 6084-9.*

Huckman MS, Fox J, Topel J. *The validity of criteria for the evaluation of cerebral atrophy by computed tomography. Radiology 1975; 116: 85-92.*

Jack CR,Jr, Lowe VJ, Senjem ML, Weigand SD, Kemp BJ, Shiung MM, et al. *C11 PiB and structural MRI provide complementary information in imaging of Alzheimer's disease and amnestic mild cognitive impairment. Brain 2008; 131: 665-80.*

Jack CR,Jr, Shiung MM, Weigand SD, O'Brien PC, Gunter JL, Boeve BF, et al. *Brain atrophy rates predict subsequent clinical conversion in normal elderly and amnestic MCI. Neurology 2005; 65: 1227-31.*

Jack CR,Jr, Shiung MM, Gunter JL, O'Brien PC, Weigand SD, Knopman DS, et al. *Comparison of different MRI brain atrophy rate measures with clinical disease progression in AD. Neurology 2004a; 62: 591-600.*

Jack CR,Jr, Shiung MM, Gunter JL, O'Brien PC, Weigand SD, Knopman DS, et al. Comparison of different MRI brain atrophy rate measures with clinical disease progression in AD. Neurology 2004b; 62: 591-600.

Jack CR,Jr, Bernstein MA, Fox NC, Thompson P, Alexander G, Harvey D, et al. The Alzheimer's disease neuroimaging initiative (ADNI): MRI methods. J Magn Reson Imaging 2008; 27: 685-91.

Jagust W. Molecular neuroimaging in Alzheimer's disease. NeuroRx 2004; 1: 206-12.

Kantarci K, Jack CR,Jr. Quantitative magnetic resonance techniques as surrogate markers of Alzheimer's disease. NeuroRx 2004; 1: 196-205.

Katz R. Biomarkers and surrogate markers: An FDA perspective. NeuroRx 2004; 1: 189-95.

Klunk WE, Engler H, Nordberg A, Wang Y, Blomqvist G, Holt DP, et al. Imaging brain amyloid in Alzheimer's disease with pittsburgh compound-B. Ann Neurol 2004; 55: 306-19.

Knopman DS, DeKosky ST, Cummings JL, Chui H, Corey-Bloom J, Relkin N, et al. Practice parameter: Diagnosis of dementia (an evidence-based review). report of the quality standards subcommittee of the american academy of neurology. Neurology 2001; 56: 1143-53.

Langbaum JB, Chen K, Lee W, Reschke C, Bandy D, Fleisher AS, et al. Categorical and correlational analyses of baseline fluorodeoxyglucose positron emission tomography images from the Alzheimer's disease neuroimaging initiative (ADNI). Neuroimage 2009; 45: 1107-16.

Lehericy S, Marjanska M, Mesrob L, Sarazin M, Kinkingnehun S. Magnetic resonance imaging of Alzheimer's disease. Eur Radiol 2007; 17: 347-62.

Luxenberg JS, Haxby JV, Creasey H, Sundaram M, Rapoport SI. Rate of ventricular enlargement in dementia of the Alzheimer type correlates with rate of neuropsychological deterioration. Neurology 1987; 37: 1135-40.

Mahley RW. Apolipoprotein E: Cholesterol transport protein with expanding role in cell biology. Science 1988; 240: 622-30.

McKhann G, Drachman D, Folstein M, Katzman R, Price D, Stadlan EM. Clinical diagnosis of Alzheimer's disease: Report of the NINCDS-ADRDA work group under the auspices of department of health and human services task force on Alzheimer's disease. Neurology 1984; 34: 939-44.

Moffat SD, Szekely CA, Zonderman AB, Kabani NJ, Resnick SM. Longitudinal change in hippocampal volume as a function of apolipoprotein E genotype. Neurology 2000; 55: 134-6.

Moller HJ, Graeber MB. The case described by alois Alzheimer in 1911. historical and conceptual perspectives based on the clinical record and neurohistological sections. European Archives of Psychiatry & Clinical Neuroscience 1998; 248: 111-22.

Mosconi L, Pupi A, De Leon MJ. Brain glucose hypometabolism and oxidative stress in preclinical Alzheimer's disease. Ann N Y Acad Sci 2008; 1147: 180-95.

Mosconi L, Brys M, Glodzik-Sobanska L, De Santi S, Rusinek H, de Leon MJ. Early detection of Alzheimer's disease using neuroimaging. Exp Gerontol 2007; 42: 129-38.

Mount C, Downton C. Alzheimer disease: Progress or profit?. Nat Med 2006; 12: 780-4.

Nordberg A. PET imaging of amyloid in Alzheimer's disease. Lancet Neurology 2004; 3: 519-27.

O'Brien JT. Role of imaging techniques in the diagnosis of dementia. Br J Radiol 2007; 80: S71-7.

Petersen RC, Stevens JC, Ganguli M, Tangalos EG, Cummings JL, DeKosky ST. Practice parameter: Early detection of dementia: Mild cognitive impairment (an evidence-based review). report of the quality standards subcommittee of the american academy of neurology. Neurology 2001; 56: 1133-42.

Petersen RC, Smith GE, Waring SC, Ivnik RJ, Tangalos EG, Kokmen E. Mild cognitive impairment: Clinical characterization and outcome. Arch Neurol 1999; 56: 303-8.

Petersen RC, Doody R, Kurz A, Mohs RC, Morris JC, Rabins PV, et al. Current concepts in mild cognitive impairment. Arch Neurol 2001; 58: 1985-92.

Petersen RC, Thomas RG, Grundman M, Bennett D, Doody R, Ferris S, et al. Vitamin E and donepezil for the treatment of mild cognitive impairment. N Engl J Med 2005; 352: 2379-88.

Petrovitch H, White LR, Ross GW, Steinhorn SC, Li CY, Masaki KH, et al. Accuracy of clinical criteria for AD in the honolulu-asia aging study, a population-based study. Neurology 2001; 57: 226-34.

Rapoport SI. Multimodal in vivo brain imaging in Alzheimer's disease: Diagnosis, characteristics, and mechanisms. In: Heston LL, editor. Progress in Alzheimer's Disease and Similar Conditions. New York: American Psychiatric Pub; 1997. p. 35-69.

Ridha BH, Anderson VM, Barnes J, Boyes RG, Price SL, Rossor MN, et al. Volumetric MRI and cognitive measures in Alzheimer disease. J Neurol 2008; 255: 567-74.

Rose SE, Janke AL, Chalk JB. Gray and white matter changes in Alzheimer's disease: A diffusion tensor imaging study. J Magn Reson Imaging 2008; 27: 20-6.

Saha PK, Udupa JK, Odhner D. Scale-based fuzzy connected image segmentation: Theory, algorithms, and validation. CVIU 2000; 77: 145-74.

Sanchez JL, Rodriguez M, Carro J. Influence of cognitive reserve on neuropsychologic functioning in Alzheimer's disease type sporadic in subjects of spanish nationality. Neuropsychiatry, Neuropsychology, & Behavioral Neurology 2002; 15: 113-22.

Scheffler K, Lehnhardt S. Principles and applications of balanced SSFP techniques. Eur Radiol 2003; 13: 2409-18.

Scheltens P, Fox N, Barkhof F, De Carli C. Structural magnetic resonance imaging in the practical assessment of dementia: Beyond exclusion. Lancet Neurology 2002; 1: 13-21.

Schmechel DE, Saunders AM, Strittmatter WJ, Crain BJ, Hulette CM, Joo SH, et al. Increased amyloid beta-peptide deposition in cerebral cortex as a consequence of apolipoprotein E genotype in late-onset Alzheimer disease. Proc Natl Acad Sci U S A 1993; 90: 9649-53.

Schott JM, Price SL, Frost C, Whitwell JL, Rossor MN, Fox NC. Measuring atrophy in Alzheimer disease: A serial MRI study over 6 and 12 months. Neurology 2005; 65: 119-24.

Schuff N, Zhu XP. Imaging of mild cognitive impairment and early dementia. Br J Radiol 2007; 80: S109-14.

Shaw LM. PENN biomarker core of the Alzheimer's disease neuroimaging initiative. NeuroSignals 2008; 16: 19-23.

Shear PK, Sullivan EV, Mathalon DH, Lim KO, Davis LF, Yesavage JA, et al. Longitudinal volumetric computed tomographic analysis of regional brain changes in normal aging and Alzheimer's disease. Arch Neurol 1995; 52: 392-402.

Silbert LC, Quinn JF, Moore MM, Corbridge E, Ball MJ, Murdoch G, et al. Changes in premorbid brain volume predict Alzheimer's disease pathology. Neurology 2003; 61: 487-92.

Sjogren M, Vanderstichele H, Agren H, Zachrisson O, Edsbagge M, Wikkelso C, et al. Tau and Abeta42 in cerebrospinal fluid from healthy adults 21-93 years of age: Establishment of reference values. Clin Chem 2001; 47: 1776-81.

Small GW, Bookheimer SY, Thompson PM, Cole GM, Huang SC, Kepe V, et al. Current and future uses of neuroimaging for cognitively impaired patients. Lancet Neurology 2008; 7: 161-72.

Small GW, Kepe V, Ercoli LM, Siddarth P, Bookheimer SY, Miller KJ, et al. PET of brain amyloid and tau in mild cognitive impairment. N Engl J Med 2006; 355: 2652-63.

Swartz RH, Black SE, St George-Hyslop P. Apolipoprotein E and Alzheimer's disease: A genetic, molecular and neuroimaging review. Canadian Journal of Neurological Sciences 1999; 26: 77-88.

Temple R. Are surrogate markers adequate to assess cardiovascular disease drugs?. JAMA 1999; 282: 790-5.

Thompson PM, Hayashi KM, De Zubicaray GI, Janke AL, Rose SE, Semple J, et al. Mapping hippocampal and ventricular change in Alzheimer disease. Neuroimage 2004; 22: 1754-66.

U.S. National Institute of Health. ClinicalTrials.gov search for "Alzheimer". ClinicalTrials gov May 2009; May 2009: 40.

Vas CJ, Rajkumar S, Tanyakitipisal P, Chandra V. Alzheimer's disease: The brain killer, world health organization. 2001: 1-16.

Visser PJ, Scheltens P, Pelgrim E, Verhey FR, Dutch ENA-NL-01 Study G. Medial temporal lobe atrophy and APOE genotype do not predict cognitive improvement upon treatment with rivastigmine in Alzheimer's disease patients. Dementia & Geriatric Cognitive Disorders 2005; 19: 126-33.

Wahlund LO, Julin P, Lannfelt L, Lindqvist J, Svensson L. Inheritance of the ApoE epsilon4 allele increases the rate of brain atrophy in dementia patients. Dementia & Geriatric Cognitive Disorders 1999; 10: 262-8.

Walter SD, Eliasziw M, Donner A. Sample size and optimal designs for reliability studies. Stat Med 1998; 17: 101-10.

Wang D, Chalk JB, Rose SE, de Zubicaray G, Cowin G, Galloway GJ, et al. MR image-based measurement of rates of change in volumes of brain structures. part II: Application to a study of Alzheimer's disease and normal aging. Magn Reson Imaging 2002; 20: 41-8.

Wilcock GK, Lilienfeld S, Gaens E. Efficacy and safety of galantamine in patients with mild to moderate Alzheimer's disease: Multicentre randomised controlled trial. galantamine international-1 study group. BMJ 2000; 321: 1445-9.

Wilks , S. Clinical notes on atrophy of the brain. J. Ment. Sci. 1864; 10: 10-19.

Wimo A, Jonsson L, Winblad B. An estimate of the worldwide prevalence and direct costs of dementia in 2003. Dementia & Geriatric Cognitive Disorders 2006; 21: 175-81.

Winblad B, Palmer K, Kivipelto M, Jelic V, Fratiglioni L, Wahlund LO, et al. Mild cognitive impairment--beyond controversies, towards a consensus: Report of

the international working group on mild cognitive impairment. J Intern Med 2004; 256: 240-6.

Ye S, Huang Y, Müllendorff K, Dong L, Giedt G, Meng E, et al. Apolipoprotein (apo) E4 enhances amyloid β peptide production in cultured neuronal cells: ApoE structure as a potential therapeutic target. Proc Natl Acad Sci U S A 2005; 102: 18700-5.

Chapter 2

VENTRICULAR ENLARGEMENT AS A POSSIBLE MEASURE OF ALZHEIMER'S DISEASE PROGRESSION VALIDATED USING THE ALZHEIMER'S DISEASE NEUROIMAGING INITIATIVE DATABASE

A version of this chapter has been published (Sean M. Nestor, Raul Rupsingh, Michael Borrie, Matthew Smith, Vittorio Accomazzi, Jennie L. Wells, Jennifer Fogarty, Robert Bartha, and the Alzheimer's Disease Neuroimaging Initiative. *Brain.* 2008 131(9):2443-2454.)

2.1 INTRODUCTION

Brain tissue atrophy rates measured on serial magnetic resonance imaging (MRI) scans may provide an objective and quantitative method to examine neuropathological changes associated with mild cognitive impairment (MCI) and Alzheimer's disease (AD) (Bradley, et al. 2002, Fox, et al. 2000, Jack, et al. 2004a, Schott, et al. 2005, Wang, et al. 2002). Serial MRI techniques that measure neurodegeneration principally focus on volumetric analysis of the hippocampus (Devanand, et al. 2007, Jack, et al. 1997, Jack, et al. 2004a, Leinsinger, et al. 2003), whole brain (Fox and Freeborough. 1997, Fox, et al. 2000, Jack, et al. 2004a, Schott, et al. 2005, Smith, et al. 2002) and ventricles (Bradley, et al. 2002, Carmichael, et al. 2007, Fleisher, et al. 2008, Giesel, et al. 2006, Jack, et al. 2004b, Schott, et al. 2005, Silbert, et al. 2003, Thompson, et al. 2004, Wang, et al. 2002). Hippocampal volumetric analysis typically involves manual or semi-manual tracing techniques (Giesel, et al. 2006) that require a significant amount of time and interaction from experienced operators, increasing costs and decreasing reproducibility. Conversely, measurement of cerebral ventricular volume is amenable to robust automatic segmentation due to the sharp contrast between the signal intensity of cerebral spinal fluid (CSF) in the ventricles and surrounding tissue in T_1-weighted MRI images. Moreover, the

position of the ventricles near the centre of the brain places this structure near the magnet isocentre. As a result, geometric distortions across the ventricle due to gradient non-linearities are minimized.

The use of cerebral ventricular volume as a measure of AD progression is supported by several studies. Hemispheric atrophy rates, measured by ventricular enlargement, correlate more strongly with changes on cognitive tests than medial temporal lobe (MTL) atrophy rates (Jack, et al. 2004a), and capture significant variation between NEC and subjects with MCI, and AD (Bradley, et al. 2002, Jack, et al. 2005, Schott, et al. 2005). This sensitivity occurs, in part, because portions of the lateral ventricles are adjacent to MTL structures that atrophy notably in the preclinical stages of dementia (Ferrarini, et al. 2006, Giesel, et al. 2006). The rate of ventricular volume change is also highly correlated with an increase in senile plaques and neurofibrillary tangles (Silbert, et al. 2003) . Previously reported sample sizes required to detect meaningful reductions from the expected rate of annual change were markedly lower when using lateral ventricular volumes compared to psychometric, MTL and whole brain MR measurements (Fox, et al. 2000, Jack, et al. 2004a, Schott, et al. 2005). Anatomical measurements such as ventricle volume are likely to provide complementary information to neurocognitive testing, and provide insight into the mechanisms of disease modifying therapies. It may be possible to use such measures to select subjects likely to respond to specific disease-modifying therapies and subsequently assess the biological efficacy of these treatments.

The allele ε4 of the apolipoprotien ε (APOE) gene has been well established as a primary risk factor for AD, and APOE has previously been associated with increased neurofibrillary tangles, increased plaque burden (Schmechel, et al. 1993), 19, and cognitive decline (Bizzarro, et al. 2005, Blesa, et al. 2006) . In addition, previous retrospective studies (Farlow, et al. 2004) and a few prospective studies (Bizzarro, et al. 2005, Frankfort, et al. 2007) of cholinesterase inhibitor treatment of AD have noted differential therapeutic responses between APOE genotypes. However, associations between APOE genotype and measures of structural rates of change are not well characterized in subjects with MCI and AD. Further, the majority of studies evaluating genotype and brain tissue atrophy are cross-sectional (Bigler, et al. 2000a, den Heijer, et

al. 2002, Jack, et al. 1998); although one previous longitudinal study examined the interaction between ventricular enlargement and genotype in a small sample of AD subjects using manual quantification methods (Wahlund, et al. 1999). Thus, there is a strong rationale for the characterization of differences in ventricular enlargement between genotypes, and to determine the number of subjects required to detect a change in the expected natural history of ventricular enlargement.

Despite the evidence supporting the use of ventricular volume as a measure of disease progression in AD and MCI, there are only two studies of ventricular volume change over short time intervals (less than 1 year) (Bradley, et al. 2002, Schott, et al. 2005). However, these studies were from single centres, were limited by the small sample sizes used, did not compare structural measures to neurocognitive scores, did not include an MCI group and did not examine differences in APOE genotype (Bradley, et al. 2002, Schott, et al. 2005). In the current study, a large image dataset compiled from over forty-eight centres was obtained for NEC, MCI (including a subset of MCI subjects that converted to AD after six months), and AD subjects from the Alzheimer's Disease Neuroimaging Initiative (ADNI). The primary goal of ADNI is to test whether serial MRI, positron emission tomography, other biological markers and clinical and neurocognitive assessment can, alone or in combination, measure the progression of MCI and early AD. Determination of sensitive and specific markers of very early AD progression is intended to aid researchers and clinicians to develop new treatments and monitor their effectiveness, as well as lessen the time and cost of clinical trials.

The primary purpose of the current study was to examine the cross-sectional and longitudinal ventricular volume differences between and within NEC, MCI and AD subjects after only six months in a multi-centre study. The secondary objectives were to determine (i) whether ventricular dilatation in AD is sensitive to disease progression after six months, (ii) whether there is a difference in the rate of ventricular enlargement between APOE genotypes, (iii) the number of subjects necessary to detect a meaningful change from the natural history of ventricular enlargement with respect to genotype, and (iv) whether the rate of ventricular enlargement over six months correlates with the cognitive measures usually used in AD clinical trials including the Mini Mental State

Exam (MMSE) (Folstein, et al. 1975), and the Alzheimer's Disease Assessment Scale-cognitive (ADAS-cog) test scores (Rosen, et al. 1984). We hypothesized that ventricular dilatation after six months would discriminate NEC, MCI, MCI to AD progressors, and AD patients, and be a more sensitive measure of disease progression than cognitive scores.

2.2 MATERIALS AND METHODS

2.2.1 SUBJECTS

Data used in the preparation of this article were obtained from the ADNI database (www.loni.ucla.edu\ADNI). The ADNI was launched in 2003 by the National Institute on Aging (NIA), the National Institute of Biomedical Imaging and Bioengineering (NIBIB), the Food and Drug Administration (FDA), pharmaceutical companies and non-profit organizations, as a $63 million, 5-year public–private partnership. The principal investigator of this initiative is Michael W. Weiner, MD, VA Medical Centre and University of California–San Francisco. ADNI is the result of efforts of many co-investigators from a broad range of academic institutions and private corporations, and subjects have been recruited from over 50 sites across the US and Canada. The initial goal of ADNI was to recruit 800 adults, ages 55 to 90, to participate in the research; approximately 200 cognitively normal older subjects to be followed for three years, 400 people with MCI to be followed for 3 years, and 200 people with early AD to be followed for 2 years. Written informed consent was obtained from patients or their families. Data acquisition was approved by the local ethics review board at each participating site.

The current study included 504 subjects from the ADNI database that had both baseline and six-month follow-up data available at the time of analysis (August–September 2007), including 105 AD, 247 MCI and 152 NEC subjects. The subject selection protocol and clinical evaluation has been previously reported (Alzheimer's Disease Neuroimaging Initiative, 2008). To summarize, at baseline, classification of the diagnostic group was based on clinical judgment assimilating medical history, clinical evaluation and several neurocognitive tests. At six-month, follow-up subjects were evaluated in a multiple-step

procedure, to determine whether MCI and NEC remained appropriate diagnoses or whether the patient had progressed to possible or probable AD according to established NINCDS/ADRDA criteria. Participants were screened with the modified Hachinski scale to exclude persons with marked cerebrovascular disease and/or multi-infarct dementia. Persons scoring >4 on the modified Hachinski scale were excluded at screening from ADNI. Participants with a history of a clinical stroke were also excluded at screening from ADNI. White matter T_2/Proton Density MRI hyper intensity volume was not an exclusion criterion.

All images selected from the ADNI database were acquired on 1.5 Tesla General Electric (GE) Medical Systems (N = 262), Philips (N = 11), or Siemens (N = 207), MR clinical scanners in accordance with the standard ADNI MR imaging protocol (Jack *et al.*, 2008✦). In addition, a subset of individuals had scans on a GE system at baseline and then a Siemens system at six months (N = 24). Measurements of ventricular volume were made from 3D T_1-weighted magnetization prepared rapid acquisition gradient echo (MP-RAGE) images acquired in the sagittal plane (for detailed pulse sequence parameters see (Jack, et al. 2008). Raw images uncorrected by ADNI site-specific phantom calibration results were used. For the scans completed on the GE and Siemens systems there was no N3 correction, B_1 correction, gradient warping correction, or phantom-based scaling. The scans completed on the Philips systems were automatically B_1 corrected on the scanner.

2.2.2 PSYCHOMETRIC ASSESSMENTS

Psychometric assessments were acquired at both baseline and six months for all subjects in each of the three groups. Although there were several tests administered to subjects in the ADNI protocol, two of these tests were chosen for this study based on their use in multicentre studies and previously demonstrated correlation with structural MR measures at intervals greater than or equal to one year (Duarte, et al. 2006, Jack, et al. 2004a, Thompson, et al. 2004). The Alzheimer's Disease Assessment Scale-cognitive subscale scores (ADAS-cog) (Rosen, et al. 1984) were acquired to test for associations with volumetric measures, as these cognitive scores are the primary endpoints for dementia trials (Fox NC. Black RS. Gilman S. Rossor MN. Griffith SG. Jenkins L. Koller M.

AN1792(QS-21)-201 Study. 2005). The Mini-Mental State Examination (MMSE) (Folstein, et al. 1975) was used because of its ubiquitous application in clinical settings.

2.2.3 VENTRICULAR VOLUME MEASUREMENT

All volumetric analysis was performed on a Windows XP workstation using the semi-automated software Brain Ventricle Quantification (BVQ) (Accomazzi, et al.) developed by Cedara Software and refined collaboratively by Cedara Software and Robarts Research Institute. A single researcher (S.M.N.), who was blinded to the age, gender, all clinical information, diagnostic group and chronological ordering within each scan pair, performed all volumetric analyses of the ADNI data. Operator-selected seed points were placed in each lateral ventricle and a region-growing algorithm automatically expanded the seed points within the 3D space of the image to the margin of the periventricular tissue. The region-growing procedure combined image intensity and shape analysis (using morphological operators) and was specifically optimized for the segmentation of the lateral ventricles (Accomazzi, et al. , Saha, et al. 2000). The lateral ventricles were then automatically rendered in three dimensions and in the coronal, sagittal and axial planes for inspection (Figure 2-1). In certain cases extraneous anatomical volumes (usually third and fourth ventricular volumes) were removed by identifying the tissue connecting the ventricle proper and the extraneous volumes. BVQ then automatically removed the extraneous tissue to the border of the lateral ventricles. This type of minimal manual interaction was required in approximately one-third of all subjects. Each 3D volume took approximately 1 min to segment. An additional minute was needed for analyses that require semi-automated editing, usually to remove volume that had been attributed to the third ventricle.
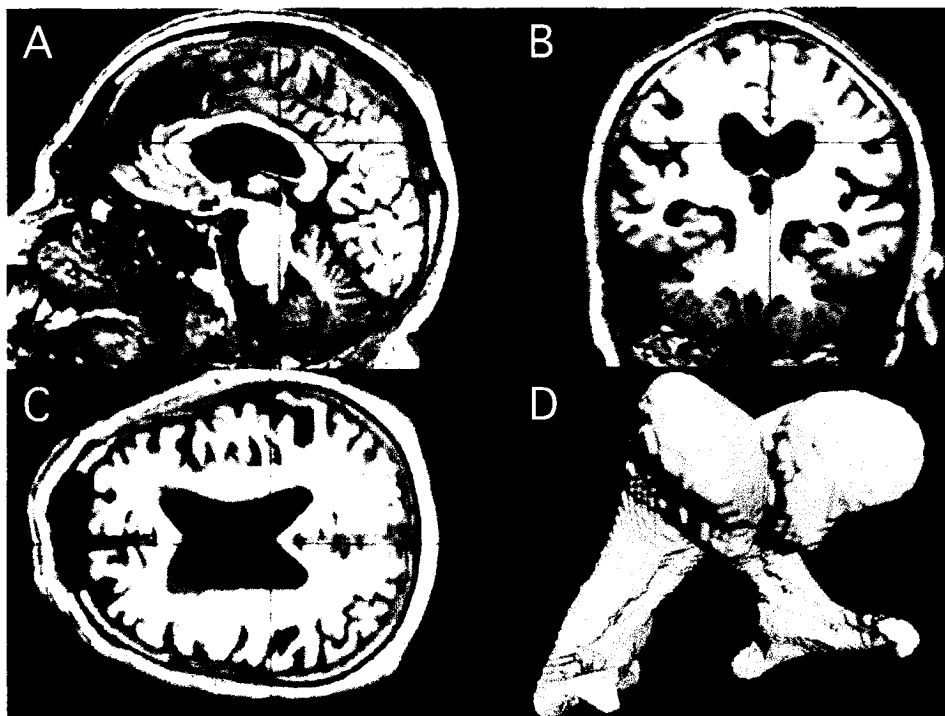
Figure 1: Sagittal (A), coronal (B), and transverse (C) T_1-weighted MRI images of one subject with the pixels assigned to the lateral ventricles by the Brain Ventricle Quantification software colored in red. A three-dimensional rendered view of the ventricle from this subject (D) is used for quality control purposes.

2.2.4 STATISTICAL ANALYSIS

Automatic volumetric measurement stability was assessed through a repeatability analysis. Intra-rater and inter-rater correlation coefficients (ICC) were determined from a set of 27 subjects, which consisted of 3 groups (AD, MCI, NEC) of 9 subjects randomly selected from the ADNI database. This sample size was chosen to calculate ICC with a significance level of 0.05 and 80% power using two time points (intra-rater) and two operators (inter-rater)(Walter, et al. 1998). Two operators (S.M.N., R.R.) performed volume measurements at baseline and again one week later on all 27 datasets. All ICC calculations were performed using a 1-way ANOVA model in SAS 9.1 (SAS Institute Inc., North Carolina). A subset of data were also examined to determine whether the incorporation of the available image corrections (gradient warp correction, B_1 correction, N3 correction and phantom scaling correction) had an appreciable effect on ventricle

volume measurement. To perform the analysis, ventricle volumes were segmented on 28 randomly chosen subjects (NEC = 10, MCI = 11, AD = 7) using phantom-scaled/optimized images (including gradient warp correction, B_1 correction and N3 correction) and the raw images, both at baseline and at six-month follow-up.

The rate of ventricular enlargement was computed in each subject by taking the absolute difference between six-month and baseline volumetric measurements, as well as by taking the percent change from baseline ventricle volume. Normalization to whole-brain volume was not necessary because each subject served as their own control (Jack, et al. 2004a). Further, normalization of volumes to other brain structures was not performed prior to analysis of cross-sectional ventricular volumes, as Carmichael *et al.* have previously demonstrated that this normalization does not significantly affect results (Carmichael, et al. 2007).

Statistical analysis was performed using SPSS 15 (SPSS Incorporated, Chicago Illinois). The primary analysis consisted of comparisons between all groups (NEC, MCI and AD) on baseline and longitudinal measures, and within groups for longitudinal measures. An analysis of covariance was computed by the general linear model, and Bonferroni tests to adjust for multiple comparisons were conducted for all between group post-hoc investigations. Age, education and scan interval were included as covariates where appropriate based on an ANCOVA. A repeated measures *t*-test was applied for each within group analysis (changes in MMSE, ADAS-cog and ventricular volume) for all groups and these nine tests were Bonferroni corrected for multiple comparisons.

For secondary analyses, Levene's test was used to analyse homogeneity of variance between ventricular volumes and rates of enlargement between all groups. All statistical tests were two sided, with significance set at the 0.05 level. No secondary analyses were corrected for multiple comparisons. Associations between baseline cognitive scores, rate of cognitive change, baseline ventricular volumes and ventricular enlargement were tested using linear Pearson correlations for each subgroup.

The MCI group was dichotomized by grouping subjects who progressed to a clinical diagnosis of AD after six months and subjects that remained stable. Differences between groups were assessed by an independent sample *t*-test and longitudinal change was assessed with a repeated measures *t*-test. In addition, each group (NEC, MCI, AD) was dichotomized into ε4– (ε2/ ε3 heterozygote or ε2/ ε3 homozygote) and ε4+ (ε4 homozygote or ε4 heterozygote) subjects for consistency with previous studies (Bigler, et al. 2000a, Blesa, et al. 2006, Farlow, et al. 2004). The ventricular and cognitive change measures were compared between strata within each group (NEC, MCI and AD) using an independent sample *t*-test. All *t*-tests were two sided.

Sample size calculations were performed using a conventional protocol employed by Fox *et al.* (Equation 1 in (Fox, et al. 2000)) for cerebral atrophy. This calculation assumed that there were no differences in standard deviations between groups and that detection of a 20% change is derived with 90% power at a 5% level of significance, for two-sided significance tests.

2.3 RESULTS

Ventricular volume measurements using the BVQ software (Figure 2-1) were highly reproducible (Table 2-1). The intra-operator and inter-operator correlation coefficients were greater than 0.98 (Table 2-1). The ICC was also high for both baseline (0.998) and six-month (0.999) ventricle volumes when comparing volumes derived from raw images and those derived from the scaled and corrected images. A chi-squared test showed that the different types of scanners were equally distributed in the three primary study groups. There was no significant main effect of site for ventricular rates of change. In addition, there was no statistically significant interaction between group and site for measures of six-month ventricular change.

Table 2-1. ICC Reliability results for semi-automated (Ventricular volume) Brain Ventricle Quantification measurements

Reliability Measure	ICC	[95% CI]
Intra-Operator 1	0·99997	[0·99994-0·99999]
Intra-Operator 2	0·98098	[0·95935-0·99131]
Inter-Operator at Baseline	0·99977	[0·99950-0·99989]
Inter-Operator at Follow-up	0·98100	[0·95939-0·99132]

ICC = Inter/Intra rater correlation coefficient, CI = Confidence interval

Demographic information is provided in Table 2-2. No subjects had a lumbar puncture before their MR scan. Scan interval was not significantly different between groups and did not influence the outcome of the group-wise comparisons. Specifically, the average scan interval for NEC ± SD = 7.0 ± 0.1 months, MCI group = 7.1 ± 0.1 months, and for subjects with AD = 6.8 ± 0.1 months. There was a gender difference found within groups. Specifically, there were significantly more male subjects within both MCI ($P < 0.0001$) and AD ($P = 0.0248$) groups. However, there were no significant differences in gender between groups. There was no significant difference in age or education between groups. More than half of the patients with MCI were on dementia medication. There were 98 subjects in the AD group on cholinesterase inhibitor therapy, and there were 61 subjects on Memantine.

Table 2-2. Demographic Data and cognitive scores for the three Defined Groups of Subjects

Group	NEC			MCI					AD		
	ε4-	ε4+	All Subjects	Stable	Converter	ε4-	ε4+	All Subjects	ε4-	ε4+	All Subjects
Sample Size	109	43	152	228	18	110	136	246	30	74	104
Age (years) (mean ± SD)	76.5 ± 5.2	76.1 ± 5.2	76.4 ± 5.2	74.7 ± 7.7	75.0 ± 7.3	75.7 ± 8.4	74.0 ± 6.9	74.7 ± 7.3	77.7 ± 8.6	73.8 ± 6.5	74.9 ± 15.0
Sex (male)	56	25	81	148	3	77	85	165	13	42	64
Education (years) (mean ± SD)	16 ± 3	16 ± 3	16 ± 3	16 ± 3	16 ± 4	16 ± 3	16 ± 3	16 ± 3	16 ± 3	15 ± 3	15 ± 3
MMSE at Baseline (mean ± SD)	29.1 ± 1.0	29.2 ± 0.8	29.1 ± 0.9	27.0 ± 1.8	25.9 ± 1.6	27.1 ± 1.8	26.7 ± 1.8	26.9 ± 1.8	23.5 ± 1.9	23.3 ± 1.9	23.3 ± 1.9
ΔMMSE (mean ± SD)	-0.1 ± 1.2	-0.09 ± 1.3	-0.1 ± 1.2	-0.5 ± 2.2	-1.7 ± 2.2	-0.3 ± 2.2	-0.9 ± 2.4	-0.6 ± 2.3	0.2 ± 3.0	-1.3 ± 3.3	-0.9 ± 3.3
ADAS-cog at Baseline (mean ± SD)	5.9 ± 3.0	6.8 ± 3.5	6.2 ± 3.2	11.5 ± 4.3	13.2 ± 5.2	10.8 ± 4.3	12.4 ± 4.34	11.7 ± 4.4	15.6 ± 5.2	18.3 ± 5.9	17.5 ± 5.8
ΔADAS-cog (mean ± SD)	0.0 ± 2.9	0.1 ± 3.8	0.0 ± 3.2	0.6 ± 4.1	1.2 ± 4.7	0.8 ± 4.1	0.4 ± 4.1	0.6 ± 4.2	2.0 ± 4.0	2.6 ± 4.2	2.4 ± 4.2

Apoe E4 = Apolipoprotein gene, ε4+= at least one ε4 allele, ε4- = no ε4 allele; NEC = Normal Elderly Control, MCI = Mild Cognitive Impairment, AD = Alzheimer Disease; * Represent approximations, as not all subjects had start month data available; † Alzheimer's Disease Assessment Scale-cognitive subscale (ADAS-cog): 2 missing in MCI group; ‡ Mini Mental State Exam (MMSE): 2 missing at baseline in MCI group

There were no early terminations among the subjects examined in this study at six months. However, two subjects did not have an MRI scan at six-month follow-up (MCI = 1, AD = 1) and were not included in the longitudinal analysis; two subjects did not have an MMSE administered at six months (MCI = 2); two subjects did not have the ADAS-cog administered at six months (MCI = 2).

2.3.1 LONGITUDINAL AND CROSS-SECTIONAL VENTRICULAR VOLUME MEASUREMENTS

Total ventricular volume and the rate of change over six months are reported in Table 2-3. At baseline, ventricular volume was significantly larger in both AD subjects ($P < 0.0001$) and MCI subjects ($P = 0.0001$) compared to the NEC group. All groups, including NEC, showed a significant increase in absolute and percent ventricular volume after six months (Table 2-3). The AD group had a significantly greater absolute ventricular enlargement than both subjects with MCI ($P = 0.0004$) and NEC ($P < 0.0001$). Patients with MCI also had a significantly greater rate of enlargement than NEC ($P = 0.0001$). Similarly, when analysing ventricular change as a percentage of baseline ventricular volume, the AD group had a significantly greater rate than the NEC group ($P < 0.0001$) and MCI group ($P = 0.0004$), and the MCI group had a significantly greater rate than controls ($P = 0.0034$). The cross-sectional variance of ventricular volumes in the AD group at baseline was significantly greater than the NEC group ($P = 0.0015$). The MCI group was not significantly different from NEC and AD for cross-sectional variance. The variance for the rate of ventricular enlargement was significantly greater in both the MCI and the AD groups compared to NEC ($P < 0.0001$).

Table 2-3. Means from 1-way ANCOVA Ventricular
Cross-sectional and longitudinal data

|	Baseline Ventricular Volume ± SD (cm^3)	Ventricular Enlargement after six months (cm^3) (mean ± SD)	Percent Ventricular Enlargement after six months from Baseline (%) (mean ± SD)	p-value*
NEC (all subjects)	38.3 ± 19.1	0·6 ± 1.4	1.5 ± 4.3	< 0·0001
MCI (all subjects)	45.8 ± 21.4	1.6 ± 2.4	3.4 ± 6.1	< 0·0001
AD (all subjects)	49.9 ± 25.3	2.6 ± 2.0	5.7 ± 4.9	< 0·0001
MCI Stable	45.6 ± 20.7	1.5 ± 2.3	3.2 ± 6.0	= 0·0031
MCI to AD Converters	48·2 ± 29·2	2·8 ± 3.4	5.5 ± 6.1	< 0·0001
NEC ε4-	37.9 ± 18.0	0.6 ± 1.3	1.5 ± 4.0	= 0.0102
NEC ε4+	39.1 ± 21.8	0.7 ± 1.7	1.7 ± 5.1	< 0·0001
MCI ε4-	47.4 ± 22.6	1.4 ± 2.7	2.7 ± 6.3	< 0·0001
MCI ε4+	44.6 ± 20.4	1.7 ± 2.1	3.9 ± 5.9	< 0·0001
AD ε4-	47.3 ± 28.0	1.8 ± 1.7	4.6 ± 4.5	< 0·0001
AD ε4+	50.9 ± 24.2	3.0 ± 2.1	6.2 ± 5.0	< 0·0001

* indicates p-values for repeated measures t-tests for two time-points (baseline and six-months); NEC = Normal Elderly Control, MCI = Mild Cognitive Impairment, AD = Alzheimer Disease, ε4- = subjects with no APOE ε4 allele, ε4+ = subjects with at least one APOE ε4 allele

2.3.2 LONGITUDINAL AND CROSS-SECTIONAL COGNITIVE MEASUREMENTS

The cognitive test results for all patient groups at baseline and six months are summarized in Table 2-2. A significant positive correlation between baseline ventricular volume and age was found within each subgroup (NEC: $r = 0.174$, $P = 0.033$, MCI: $r = 0.315$, $P < 0.0001$, AD: $r = 0.311$, $P < 0.0001$). The MCI group displayed a significant decline in MMSE scores ($P < 0.0001$) after six months. Only the ADAS-cog scores increased in the

AD group after six months ($P < 0.0001$). Within the MCI group, ventricular enlargement was significantly correlated with decline in MMSE score ($r = -0.216$, $P = 0.0007$). Further, change in ADAS-cog scores were significantly correlated with ventricular enlargement in the MCI group ($r = 0.128$, $P = 0.046$).

Eighteen subjects diagnosed with MCI at baseline, clinically progressed to AD after six months. Two-hundred-twenty-eight remained stable with MCI. Both groups had significant ventricular enlargement (Table 2-3). Progressors demonstrated significantly greater ventricular enlargement than subjects who remained stable ($P = 0.027$). There was no statistical difference in baseline ventricular volumes between MCI strata. Subjects with MCI that progressed to AD had a significantly greater rate of cognitive decline than stable subjects ($P = 0.020$), and progressors had significantly greater cognitive deficit measured at baseline on the MMSE ($P = 0.012$). There was no significant decline in MCI progressors on the ADAS-cog after six months or significant difference in rate of decline on the ADAS-cog between MCI strata after six months. However, there was a significant positive association in MCI progressors between ventricular enlargement and cognitive decline measured on the ADAS-cog ($r = 0.627$, $P = 0.0051$) (Figure 2-2).
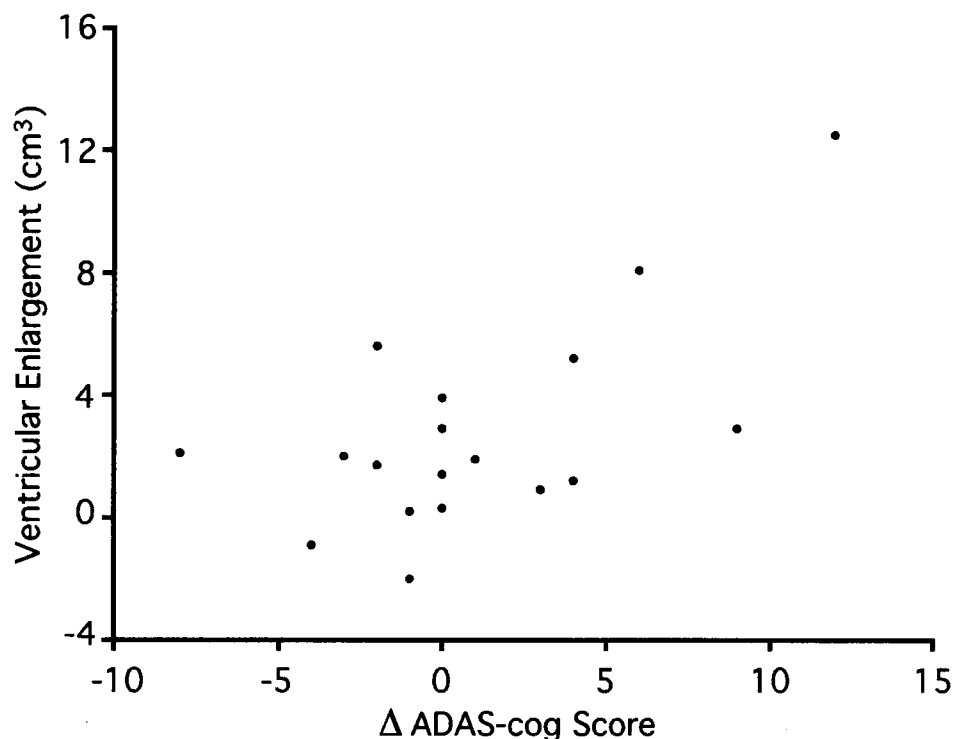
Figure 2-2. A Scatter plot of the association between absolute ventricular enlargement (cm^3) and change in score on the Alzheimer Disease Assessment – Cognitive Subscale (ADAS-cog) (an increase in score is taken as evidence of cognitive decline).

Ventricular enlargement was significantly greater in the AD ε4+ group compared to AD ε4– subjects ($P = 0.010$) (Table 2-3). However, there were no significant differences for ventricular measures realized in either the MCI or NEC genotypic groups. However, ε4+ MCI subjects had greater cognitive decline on the MMSE ($P = 0.0357$) compared to ε4– subjects. In addition, rate of change on the MMSE was significantly associated with ventricular enlargement for ε4+ subjects with MCI ($r = -0.420$, $P < 0.0001$). No other significant correlations were observed when dichotomizing for APOE genotype (Figure 2-3).
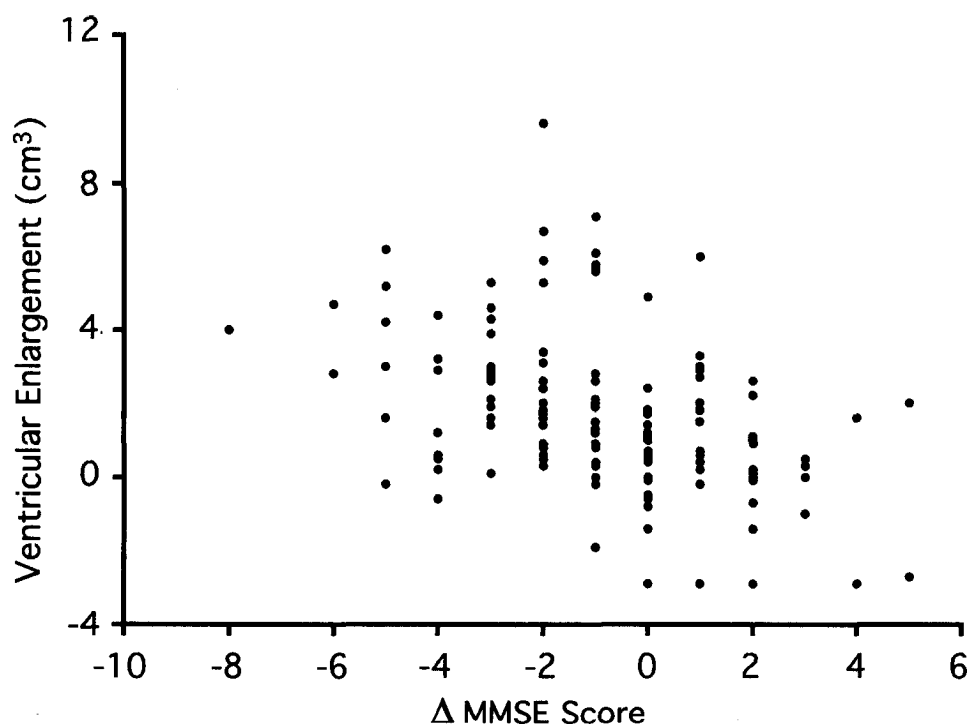
Figure 2-3. A scatter plot of the association between absolute ventricular enlargement (cm³) and change in score on the Mini Mental State Exam (MMSE) (a decline in MMSE score suggests a decline in cognition).

The estimated sample sizes required to detect a 20% change in ventricle volume, MMSE and ADAS-cog change based on the six month rate of ventricular enlargement are presented in Table 2-4. Since there were no significant differences in ventricular enlargement between MCI genotypes, sample sizes were not derived for these strata.

Table 2-4. Six-month estimated sample sizes required to detect a 20% change from the expected absolute rate of change in ventricular volumes, ADAS-cog scores, and MMSE scores.

		Lateral Ventricular	Δ MMSE Score	Δ ADAS-Cog Score
AD	**Six-Month**	342	7056	1607
AD (E4-)	**Six-Month**	468	>>20,000	2100
AD (E4+)	**Six-Month**	257	3382	1370
MCI	**Six-Month**	1180	7712	>>20,000

MMSE = Mini Mental State Exam, ADAS-cog = Alzheimer's Disease Assessment Scale –Cognitive Subscale; AD = Alzheimer Disease, MCI = Mild Cognitive Impairment

2.4 DISCUSSION

This study examined both total ventricular volume at baseline and ventricular enlargement over six months using a large ADNI subset of NEC, subjects with MCI and subjects with AD. Both AD and MCI subjects had significantly greater mean baseline ventricle volumes compared to controls. However, considerable overlap between individuals existed between all groups. Statistically significant ventricular enlargement was observed in all groups after six months. Subjects with AD had a 60% greater ventricular enlargement compared to subjects with MCI and a 4-fold greater enlargement compared to NEC measured over a six-month interval. In the MCI group, ventricular volume and ventricular enlargement were associated with baseline cognitive scores and cognitive decline, while in the AD group ventricular enlargement was associated with baseline cognitive score. After dichotomizing the MCI group based on clinical status at six months, those individuals who progressed to AD had greater ventricular enlargement and lower MMSE scores on average after six months.

Raw T_1-weighted images (without gradient warp correction, B_1 correction, N3 correction, or phantom scaling correction) were used for the analyses. Ventricle volume

measurements from these images were highly reproducible within and between raters. Additionally, comparison to scaled and corrected images using a subset of data produced very high inter-class correlation coefficients suggesting that the raw images provided comparable measurements to the phantom-scaled and corrected images–with respect to the measurement of ventricular volume. These data suggest that our ventricular volume marker is robust to scanner inhomogeneities and supports the use of either raw images or the corrected images for this metric. The robust nature of the measurement is in part due to the geographical position of the ventricles near the centre of the brain which places this structure near the magnetic isocentre where gradient non-linearities are minimized.

The primary outcome in this study is absolute ventricular change. A previous study has concluded that absolute rates of change are more statistically efficient measures than normalized change (Vickers. 2001) and demonstrated that fractional change or percent change from baseline does not correct for imbalance between groups at baseline. Percent change measures may also create a non-normally distributed statistic from normally distributed data (Vickers. 2001). In the current study, normalized ventricular change was found to be a less efficient metric, as there was more variation relative to the mean for the normalized ventricular change data in comparison to the absolute ventricular change measures.

The finding that subjects with MCI have similar total ventricular volumes to subjects with AD, suggests significant levels of atrophy may occur in the brain prior to a clinical diagnosis of dementia. Nevertheless, there was large overlap in volumes between both pathological groups and controls, which corroborates other cross-sectional volumetric studies (Table 2-5). However, only one other cross-sectional study in Table 2-5 reported baseline ventricular volume in MCI subjects (Giesel, et al. 2006). A gender difference did exist within both the MCI and AD study groups, however, there were no gender differences between groups; thus, it is unlikely that skewed gender ratios affected the volumetric results.

Table 2-5. Absolute baseline ventricular volumes and annual or annualized rate of lateral ventricular enlargement reported in the literature

Study	Sample Size			Absolute Ventricular Volume (mean ± SD)			Annual Ventricular Enlargement (mean ± SD)			Units
	NEC	MCI	AD	NEC	MCI	AD	NEC	MCI	AD	
Giesel, et al. 2006	21	21	10	27.7 ± 12.5	24.2 ± 10·1	48.4 ± 24.3	NA	NA	NA	ml
Schott, et al. 2005	38		19	31.7± 22.1	NA	52.7 ± 25.5	0.8 ± 1.4	NA	4.1 ± 2.3	ml
Ridha, et al. 2008			52[†]	NA	NA	45.6·0 ± 19.2	NA	NA	4.58 ± 3.75[α]	ml
Silbert, et al. 2003	15		24	NA	NA	NA	3.3 ± 3.5	NA	5.5 ± 3.2	cm³
Jack, et al. 2004	Stable = 40 / Converter = 15	Stable = 15 / Converter = 26	Slow Progressor = 32 / Fast Progressor = 33	NA	NA	NA	Stable: 1.7 (0.9)[‡] / Converter: 3.4 (1.6)[‡]	Stable: 2.6 (1.3)[‡] / Converter: 3.4 (2.8)[‡]	Slow Progressor: 4.3 (3.3)[‡] / Fast Progressor: 6.4 (3.7)[‡]	%
Wang, et al. 2002	14		14	~30 ± NA*		~60 ± NA*	0·8 ± NA	NA	8.2 ± NA	cm³
Current Study	152	247	105	38.3± 19.1	45.8 ± 21.4	49.9 ± 25.3	1.1 ± 2.4[α]	2.7 ± 4.0[α]	4.6 ± 3.7[α]	cm³

NEC = Normal Elderly Control, MCI = Mild Cognitive Impairment, AD = Alzheimer Disease; *estimated ventricular volume and standard deviations, [†] AD placebo group, [α] Annualized Value (absolute ventricular change/scan interval in years)

The mean rates of ventricular enlargement for the NEC and AD group in this multi-centre study are consistent with previously published single-centre measures (Table 2-5). The

MCI group had a rate of enlargement intermediate to the difference between the NEC and AD groups. The large intra-group variance in both cross-sectional and six-month longitudinal data may reflect biological differences within and between subgroups, which has been characterized in other studies (Giesel, et al. 2006, Wang, et al. 2002). Specifically, cross-sectional measures in the current study reveal relatively large variations across all groups, which suggest large morphological differences among individuals. The AD group had particularly large ventricular variation compared to NEC subjects at baseline. This result suggests that the pathology of dementia and rate of atrophy varies widely within AD subjects. In addition, there is a large variation in ventricular enlargement within pathological groups in comparison to control subjects, which is likely attributable to differential rates of disease progression (slow and fast progressors) and disease severity.

The subset of subjects with MCI at baseline who progressed to AD after six months demonstrated nearly twice the rate of ventricular enlargement compared to stable MCI subjects. Progressors presented a similar rate of enlargement to that of subjects with AD. Mild cognitively impaired subjects that progressed to AD also demonstrated cognitive decline measured by the MMSE. Thus, absolute ventricular enlargement is demonstrably sensitive to clinically measured disease progression over short intervals in a multi-centre study. This result supports the notion that longitudinal absolute measures of structural change measured over a set interval may provide more predictive value of progression from MCI to AD than cross-sectional volumes. However, a previous single centre study by Jack *et al.* with relatively small sample sizes did not show a significant difference between the percent ventricular enlargement of subjects that converted from MCI to AD and subjects with stable MCI (Jack, et al. 2004a). They did, however, see a significant percent change difference between these groups for whole brain atrophy (Jack, et al. 2004a). In the current study, the MCI progressor group did not have a significantly different change on the ADAS-cog when compared to the MCI stable group. However, decline as measured by an increase in ADAS-cog score, was moderately associated with ventricular enlargement. This suggests that as cognition worsens on global cognitive measures, there is associated macroscopic loss of brain tissue.

The current study demonstrates that AD carriers with at least one ε4 allele have a pronounced increase in ventricular enlargement, in the absence of detectable cognitive differences, in comparison to ε4- subjects. There were no differences in ventricular change between MCI genotypes; however, the rate of cognitive decline was greater for ε4+ MCI subjects. These results suggest a pronounced effect of the APOE ε4 gene on cerebral atrophy for mild AD. A recent comprehensive qualitative review lists only four previous cross-sectional studies and one longitudinal study examining the association between ventricular volume and APOE genotype (Cherbuin, et al. 2007). The only reported longitudinal study found no difference between APOE genotypes within an AD group, although it found a greater rate of enlargement in ε4 carriers with other dementias in comparison to non-carriers (Wahlund, et al. 1999); however, this study used manual methods, was based on a small sample of AD subjects and examined a younger AD group with greater cognitive deficit measured on the MMSE than the current study. The majority of studies that incorporate an AD group are cross sectional and thus fail to capture the association of APOE and dynamic structural changes in subjects with AD. Measures of change are important when considering the heterogeneity of ventricular volumes among all AD subjects at baseline. A longer follow-up interval may also demonstrate more appreciable difference in structural brain changes between MCI and NEC APOE groups.

The temporal horns of the lateral ventricles are adjacent to paralimbic tissue and demonstrably capture changes in these regions, which are pathologically susceptible during the prodromal stages of dementia (Chetelat and Baron. 2003). A previous study of surface map changes in the temporal horns of controls and subjects with AD found regional enlargement correlates to disease progression (Thompson, et al. 2004). A recent ventricular subfield analysis of subjects with AD, however, postulates there are several other hemispherical brain structures contributing to ventricular dilatation in conjunction with MTL structures (Ferrarini, et al. 2006). This result is congruous with the topographical staging of cerebral neurodegeneration delineated by Braak and Braak in subjects with AD (Braak and Braak. 1994). Hence, the total lateral ventricular measures may capture hemispherical atrophy in conjunction with MTL atrophy, which analysis of

strictly the temporal horns would exclude. These more global lateral ventricular enlargement measures, may explain the significantly greater rates of enlargement in subjects with AD compared to patients with MCI. Furthermore, one study found that a robust measure of temporal horn volume incorporated total lateral ventricular volume (Giesel, et al. 2006). Thus, total lateral ventricular volume may be the most sensitive single measure to discriminate enlargement between NEC, subjects with MCI and subjects with AD over short durations.

An important application of volumetric MRI measurements of disease progression is towards evaluating drug therapy in AD multi-centre clinical trials, and during prodromal stages of dementia, notably in subjects with MCI. In addition, measures at short intervals, for example six months, expedite the process of drug innovation. Currently, cognitive scores are used as endpoints in clinical trials. Neuroimaging is increasingly used to evaluate structural changes in response to therapeutic intervention. In the current study, the AD group had a stable mean MMSE score after six months, which may be ascribed to the efficacy of therapeutic interventions to ameliorate cognitive symptoms over short durations, as the majority of AD subjects were administered cholinesterase inhibitor therapy. However, the same group did have an increase in mean ADAS-cog score, which is a more sensitive cognitive measure. The MCI group demonstrated both a modest average increase on the ADAS-cog and decrease on the MMSE over the same time interval. Ventricular volume changes were also detected in these groups during this period. Sample sizes needed to detect ventricular enlargement for MCI subjects and AD subjects were lower than the sample sizes required when using psychometric measures to detect changes from the natural history of cognitive or functional decline (Table 2-4). The smaller sample size derived from structural measures is due to the lower variability in measures of ventricular volume compared to the change in neurocognitive scores. Moreover, high education levels and the prevalent use of cholinesterase inhibitor therapy in conjunction with the use of Memantine, may partially explain the relatively large samples required to detect a 20% reduction in the rate of decline as measured by the MMSE and ADAS-cog (Table 2-4). Thus, ventricular volume can provide complementary insight into insidious disease progression in the absence of cognitive

decline. Moreover, there is recent evidence to suggest ventricular volume may provide additive diagnostic utility to other neuroimaging measures (Jack, et al. 2008).

There are several threats to the internal validity of neurocognitive tests, in particular practice effects, that short testing intervals may exacerbate (van Belle, et al. 1990). Furthermore, certain individuals may develop greater cognitive reserves in response to longer durations of education and/or cognitively demanding occupations (Sanchez, et al. 2002), which may generate high cognitive scores despite underlying disease progression. In summary, neurocognitive measures require greater samples to detect significant cognitive decline in patients, particularly in subjects with mild AD over short intervals, whereas measurements of ventricular dilatation may provide insight into AD progression, particularly for multi-centre studies.

Furthermore, pharmacogenetic interactions may mediate the efficacy of certain therapeutic agents (Bizzarro, et al. 2005, Farlow, et al. 2004, Frankfort, et al. 2007). There are several retrospective studies (Farlow, et al. 2004) and a few prospective studies (Bizzarro, et al. 2005, Frankfort, et al. 2007) that have examined the differential cognitive response to cholinesterase inhibitors between APOE genotypes; however, the results are equivocal with varying methodologies. In addition, there is some evidence to suggest ε4+ subjects with MCI have greater cognitive response to Donepezil (Petersen, et al. 2005). Nevertheless, there are few studies examining structural brain changes between APOE genotypes in response to treatment (Bigler, et al. 2000b, Bizzarro, et al. 2005, Blesa, et al. 2006, Frankfort, et al. 2007, Visser, et al. 2005, Wilcock, et al. 2000). The current study demonstrates greater ventricular enlargement in AD subjects with an ε4+ genotype and supports the notion that dichotomizing subjects based on genotype may provide the greatest sensitivity to detect changes in the natural history of disease progression (Table 2-4). Although it is possible that temporal effects (time since diagnosis), age of sample and disease severity may alter APOE and therapeutic interactions, fewer subjects are required when examining ventricular differences, particularly for ε4+ genotypic groups. In addition, there was a significant association between ventricular enlargement and cognitive decline observed in ε4+ subjects with MCI. This association was not demonstrated in ε4– subjects, and suggests that the ε4+ subjects are driving the

significant association between ventricular enlargement and cognitive decline demonstrated when pooling all subjects with MCI.

In summary, absolute ventricular volumes and ventricular enlargement measured over a six-month interval were greater in subjects with AD and MCI compared to age-matched controls. Ventricular enlargement also demonstrated sensitivity to disease progression by way of discriminating between subjects with stable MCI and those that progressed to AD. Further, ventricular enlargement demonstrated effects of genotype on pathological phenotype in AD. As a potential measure of disease progression for multi-centre studies of both AD and MCI subjects, ventricular enlargement measures would significantly reduce the number of subjects required to demonstrate a change from the natural history of Alzheimer's disease progression.

2.5 ACKNOWLEDGEMENTS

Epidemiology & Biostatistics at the University of Western Ontario for consultation regarding statistical analysis and calculation of reliability coefficients. The original version of this manuscript was approved by the ADNI data and publication committee (DPC).

2.6 REFERENCES

Accomazzi V, Lazarowich R, Barlow CJ, Davey B. Image region segmentation system and method.

Bigler ED, Lowry CM, Anderson CV, Johnson SC, Terry J, Steed M. Dementia, quantitative neuroimaging, and apolipoprotein E genotype. Ajnr: American Journal of Neuroradiology 2000a; 21: 1857-68.

Bigler ED, Lowry CM, Anderson CV, Johnson SC, Terry J, Steed M. Dementia, quantitative neuroimaging, and apolipoprotein E genotype. Ajnr: American Journal of Neuroradiology 2000b; 21: 1857-68.

Bizzarro A, Marra C, Acciarri A, Valenza A, Tiziano FD, Brahe C, et al. Apolipoprotein E epsilon4 allele differentiates the clinical response to donepezil in Alzheimer's disease. Dementia & Geriatric Cognitive Disorders 2005; 20: 254-61.

Blesa R, Aguilar M, Casanova JP, Boada M, Martinez S, Alom J, et al. Relationship between the efficacy of rivastigmine and apolipoprotein E (epsilon4) in patients with mild to moderately severe Alzheimer disease. Alzheimer Disease & Associated Disorders 2006; 20: 248-54.

Braak H, Braak E. Morphological criteria for the recognition of Alzheimer's disease and the distribution pattern of cortical changes related to this disorder. Neurobiol Aging 1994; 15: 355,6; 379-80.

Bradley KM, Bydder GM, Budge MM, Hajnal JV, White SJ, Ripley BD, et al. Serial brain MRI at 3-6 month intervals as a surrogate marker for Alzheimer's disease. Br J Radiol 2002; 75: 506-13.

Carmichael OT, Kuller LH, Lopez OL, Thompson PM, Dutton RA, Lu A, et al. Ventricular volume and dementia progression in the cardiovascular health study. Neurobiol Aging 2007; 28: 389-97.

Cherbuin N, Leach LS, Christensen H, Anstey KJ. Neuroimaging and APOE genotype: A systematic qualitative review. Dement Geriatr Cogn Disord 2007; 24: 348-62.

Chetelat G, Baron JC. Early diagnosis of Alzheimer's disease: Contribution of structural neuroimaging. Neuroimage 2003; 18: 525-41.

den Heijer T, Oudkerk M, Launer LJ, van Duijn CM, Hofman A, Breteler MM. Hippocampal, amygdalar, and global brain atrophy in different apolipoprotein E genotypes. Neurology 2002; 59: 746-8.

Devanand DP, Pradhaban G, Liu X, Khandji A, De Santi S, Segal S, et al. Hippocampal and entorhinal atrophy in mild cognitive impairment: Prediction of Alzheimer disease. Neurology 2007; 68: 828-36.

Duarte A, Hayasaka S, Du A, Schuff N, Jahng GH, Kramer J, et al. Volumetric correlates of memory and executive function in normal elderly, mild cognitive impairment and Alzheimer's disease. Neurosci Lett 2006; 406: 60-5.

Farlow M, Lane R, Kudaravalli S, He Y. Differential qualitative responses to rivastigmine in APOE epsilon 4 carriers and noncarriers. Pharmacogenomics Journal 2004; 4: 332-5.

Ferrarini L, Palm WM, Olofsen H, van Buchem MA, Reiber JH, Admiraal-Behloul F. Shape differences of the brain ventricles in Alzheimer's disease. Neuroimage 2006; 32: 1060-9.

Fleisher AS, Sun S, Taylor C, Ward CP, Gamst AC, Petersen RC, et al. Volumetric MRI vs clinical predictors of Alzheimer disease in mild cognitive impairment. Neurology 2008; 70: 191-9.

Folstein MF, Folstein SE, McHugh PR. "Mini-mental state". A practical method for grading the cognitive state of patients for the clinician. J Psychiatr Res 1975; 12: 189-98.

Fox NC. Black RS. Gilman S. Rossor MN. Griffith SG. Jenkins L. Koller M. AN1792(QS-21)-201 Study. Effects of abeta immunization (AN1792) on MRI measures of cerebral volume in Alzheimer disease. Neurology 2005; 64: 1563-72.

Fox NC, Freeborough PA. Brain atrophy progression measured from registered serial MRI: Validation and application to Alzheimer's disease. Journal of Magnetic Resonance Imaging 1997; 7: 1069-75.

Fox NC, Cousens S, Scahill R, Harvey RJ, Rossor MN. Using serial registered brain magnetic resonance imaging to measure disease progression in Alzheimer disease: Power calculations and estimates of sample size to detect treatment effects. Arch Neurol 2000; 57: 339-44.

Frankfort SV, Appels BA, de Boer A, Tulner LR, van Campen JP, Koks CH, et al. Identification of responders and reactive domains to rivastigmine in Alzheimer's disease. Pharmacoepidemiology & Drug Safety 2007; 16: 545-51.

Giesel FL, Hahn HK, Thomann PA, Widjaja E, Wignall E, von Tengg-Kobligk H, et al. Temporal horn index and volume of medial temporal lobe atrophy using a new semiautomated method for rapid and precise assessment. AJNR Am J Neuroradiol 2006; 27: 1454-8.

Jack CR,Jr, Petersen RC, Xu YC, Waring SC, O'Brien PC, Tangalos EG, et al. Medial temporal atrophy on MRI in normal aging and very mild Alzheimer's disease.see comment. Neurology 1997; 49: 786-94.

Jack CR,Jr, Petersen RC, Xu YC, O'Brien PC, Waring SC, Tangalos EG, et al. Hippocampal atrophy and apolipoprotein E genotype are independently associated with Alzheimer's disease. Ann Neurol 1998; 43: 303-10.

Jack CR,Jr, Lowe VJ, Senjem ML, Weigand SD, Kemp BJ, Shiung MM, et al. C11 PiB and structural MRI provide complementary information in imaging of Alzheimer's disease and amnestic mild cognitive impairment. Brain 2008; 131: 665-80.

Jack CR,Jr, Shiung MM, Weigand SD, O'Brien PC, Gunter JL, Boeve BF, et al. Brain atrophy rates predict subsequent clinical conversion in normal elderly and amnestic MCI. Neurology 2005; 65: 1227-31.

Jack CR,Jr, Shiung MM, Gunter JL, O'Brien PC, Weigand SD, Knopman DS, et al. Comparison of different MRI brain atrophy rate measures with clinical disease progression in AD. Neurology 2004a; 62: 591-600.

Jack CR,Jr, Shiung MM, Gunter JL, O'Brien PC, Weigand SD, Knopman DS, et al. Comparison of different MRI brain atrophy rate measures with clinical disease progression in AD. Neurology 2004b; 62: 591-600.

Jack CR,Jr, Bernstein MA, Fox NC, Thompson P, Alexander G, Harvey D, et al. The Alzheimer's disease neuroimaging initiative (ADNI): MRI methods. J Magn Reson Imaging 2008; 27: 685-91.

Leinsinger G, Teipel S, Wismuller A, Born C, Meindl T, Flatz W, et al. Volumetric MRI for evaluation of regional pattern and progressin of neocortical degeneration in Alzheimer's disease. Radiologe 2003; 43: 537-42.

Petersen RC, Thomas RG, Grundman M, Bennett D, Doody R, Ferris S, et al. Vitamin E and donepezil for the treatment of mild cognitive impairment. N Engl J Med 2005; 352: 2379-88.

Rosen WG, Mohs RC, Davis KL. A new rating scale for Alzheimer's disease. Am J Psychiatry 1984; 141: 1356-64.

Saha PK, Udupa JK, Odhner D. Scale-based fuzzy connected image segmentation: Theory, algorithms, and validation. CVIU 2000; 77: 145-74.

Sanchez JL, Rodriguez M, Carro J. Influence of cognitive reserve on neuropsychologic functioning in Alzheimer's disease type sporadic in subjects of spanish

nationality. Neuropsychiatry, Neuropsychology, & Behavioral Neurology 2002; 15: 113-22.

Schmechel DE, Saunders AM, Strittmatter WJ, Crain BJ, Hulette CM, Joo SH, et al. *Increased amyloid beta-peptide deposition in cerebral cortex as a consequence of apolipoprotein E genotype in late-onset Alzheimer disease. Proc Natl Acad Sci U S A 1993; 90: 9649-53.*

Schott JM, Price SL, Frost C, Whitwell JL, Rossor MN, Fox NC. *Measuring atrophy in Alzheimer disease: A serial MRI study over 6 and 12 months. Neurology 2005; 65: 119-24.*

Silbert LC, Quinn JF, Moore MM, Corbridge E, Ball MJ, Murdoch G, et al. *Changes in premorbid brain volume predict Alzheimer's disease pathology. Neurology 2003; 61: 487-92.*

Smith SM, Zhang Y, Jenkinson M, Chen J, Matthews PM, Federico A, et al. *Accurate, robust, and automated longitudinal and cross-sectional brain change analysis. Neuroimage 2002; 17: 479-89.*

Thompson PM, Hayashi KM, De Zubicaray GI, Janke AL, Rose SE, Semple J, et al. *Mapping hippocampal and ventricular change in Alzheimer disease. Neuroimage 2004; 22: 1754-66.*

van Belle G, Uhlmann RF, Hughes JP, Larson EB. *Reliability of estimates of changes in mental status test performance in senile dementia of the Alzheimer type. J Clin Epidemiol 1990; 43: 589-95.*

Vickers AJ. *The use of percentage change from baseline as an outcome in a controlled trial is statistically inefficient: A simulation study. BMC Medical Research Methodology 2001; 1: 6.*

Visser PJ, Scheltens P, Pelgrim E, Verhey FR, Dutch ENA-NL-01 Study G. *Medial temporal lobe atrophy and APOE genotype do not predict cognitive improvement upon treatment with rivastigmine in Alzheimer's disease patients. Dementia & Geriatric Cognitive Disorders 2005; 19: 126-33.*

Wahlund LO, Julin P, Lannfelt L, Lindqvist J, Svensson L. *Inheritance of the ApoE epsilon4 allele increases the rate of brain atrophy in dementia patients. Dementia & Geriatric Cognitive Disorders 1999; 10: 262-8.*

Walter SD, Eliasziw M, Donner A. *Sample size and optimal designs for reliability studies. Stat Med 1998; 17: 101-10.*

Wang D, Chalk JB, Rose SE, de Zubicaray G, Cowin G, Galloway GJ, et al. *MR image-based measurement of rates of change in volumes of brain structures. part II: Application to a study of Alzheimer's disease and normal aging. Magn Reson Imaging 2002; 20: 41-8.*

Wilcock GK, Lilienfeld S, Gaens E. Efficacy and safety of galantamine in patients with mild to moderate Alzheimer's disease: Multicentre randomised controlled trial. galantamine international-1 study group. BMJ 2000; 321: 1445-9.

Chapter 3

SUMMARY AND FUTURE DIRECTIONS

3.1 ACHIEVEMENT OF THE OBJECTIVES

In this section each of the objectives outlined in the first chapter are considered. A brief summary and discussion of the relevant findings of Chapter 1 are considered. In addition, some preliminary findings from ongoing work with ADNI data are briefly described.

[I] *To refine the semi-automatic segmentation tool Brain Ventricles Quantification (BVQ)*

Chapter 1 introduced the novel region-growing ventricular segmentation tool BVQ. Optimal placement of seed points was determined and novel editing tools were introduced, which provided greater segmentation accuracy and precision. A new method of segmenting the temporal horns was also developed, which used the geometry of the ventricular trigones to delineate the posterior temporal horn border. Preliminary results are presented as ongoing work.

[II] *To test the measurement stability in healthy controls at 4.0 Tesla*

In Chapter 1, a repeatability study was reported. An experiment was devised at 4.0 Tesla, which measured ventricular volume in 10 healthy controls using a back-to-back scan protocol. Measurement stability was determined to be high. Therefore, the algorithm was robust to head placement within the scanner.

[III] *To evaluate the reliability of the BVQ algorithm*

In Chapter 2, a reliability experiment was performed on a sample of 30 ADNI participants. Two raters evaluated ventricular volumes at two different time points blind to subject and clinical data. Interrater was determined to be high for both

interrater (Baseline ICC = 0.99977 CI = 0.99950-0.99989) and intrarater (operator 1: ICC = 0.99997 CI =0·99994-0·99999; operator 2: ICC = 0·98098 CI = 0·95935-0·99131) experiments.

[IV] *To compare group-wise differences of ventricular volume and ventricular enlargement between AD, MCI and NEC subjects from a multi-centre study*

Chapter 2 demonstrated that persons with AD had a significantly greater rate of ventricular enlargement over a short interval of 6 months in comparison to persons with MCI (p = 0.0004) and NEC (p < 0.0001). Moreover, persons with MCI had a greater rate of enlargement than NEC (p = 0.0001). There was significant overlap between groups at baseline. Despite this heterogeneity, persons with AD and MCI had greater ventricular volumes than healthy controls (p<0.01). Our results are consistent with the notion that persons with AD have a greater rate of tissue loss than persons with MCI and NEC after only six months follow-up. Further, even the NEC group demonstrated tissue loss, supporting the hypothesis that tissue loss is associated with aging.

[V] *To determine if ventricular enlargement can differentiate subjects progressing from MCI to AD and those persons with MCI that remain stable at baseline*

In order to measure the sensitivity of ventricular enlargement to detect disease progression a sample of persons with MCI that converted to AD, after six months follow-up, were compared to persons remaining stable with a diagnosis of MCI. Even with a relatively small sample size of 18 progressors, significantly larger rates of ventricular enlargement were realized in progressors (p = 0.0270). Serial measures using BVQ may be a useful method to detect individuals likely to progress from MCI to AD.

[VI] *To investigate the relationship between APOE genotype and structural brain changes in subjects with NEC, MCI and AD.*

Chapter 2 compared changes in ventricular enlargement between persons with at least 1 ApoE ε4 (ε4+) allele in comparison to those without an ApoE ε4 allele (ε4-). Persons with an ε4+ genotype in the AD group had a significantly greater rate of ventricular enlargement in comparison to the AD ε4- group ($p=$ 0.010). Therefore, the ApoE ε4 allele may escalate the rate of brain tissue loss in mild AD.

[VII]   *To determine the number of subjects necessary to detect a meaningful change from the natural history of ventricular enlargement with respect to genotype.*

In Chapter 2 sample sizes were derived to detect a 20 percent reduction in the rate of ventricular enlargement and cognitive decline for ApoE genotypes within the MCI and AD groups. A 20 percent change was used to compare our results to previous studies. Sample sizes were markedly lower for volumetric measures in comparison to cognitive measures across groups and genotypes. This supports the notion that ventricular volume is a viable candidate marker to use as a secondary endpoint in an MCI or AD clinical therapeutic trial.

[VIII]   *To correlate ventricular change with neuropsychological test scores after a short six-month interval from baseline.*

In Chapter 2, the rate of cognitive decline on the MMSE and ADAS-cog were correlated with the rate of ventricular change within the NEC, MCI and AD groups. Moreover, groups were stratified by genotype and ventricular measures were associated with cognitive measures. However, there was a significant positive association in MCI progressors between ventricular enlargement and cognitive decline measured on the ADAS-cog ($r = 0.627$, $P = 0.0051$) (Figure 2-2).

In addition, rate of change on the MMSE was significantly associated with ventricular enlargement for ε4+ subjects with MCI ($r = -0.420$, $P < 0.0001$). Within the MCI group, ventricular enlargement was significantly correlated with

decline in MMSE score ($r = -0.216$, $P = 0.0007$). Further, change in ADAS-cog scores were significantly correlated with ventricular enlargement in the MCI group ($r = 0.128$, $P = 0.046$). Therefore ventricular enlargement reflects cognitive decline in MCI and AD.

3.2 WORK IN PROGRESS

3.2.1 A DIRECT COMPARISON OF VENTRICULAR VOLUMES DERIVED FROM 1.5 TESLA AND 3.0 TESLA MRI IN 115 ADNI PARTICIPANTS

Ventricular enlargement measured from T_1-weighted MRI is an indirect measure of AD progression (Carmichael, et al. 2007). Most MRI volumetric studies have assessed structural change derived from 1.5 Tesla MRI (Bradley, et al. 2002, Carmichael, et al. 2007, Ferrarini, et al. 2006, Jack, et al. 2004, Schott, et al. 2005, Silbert, et al. 2003, Wang, et al. 2002). However, 3.0 Tesla scanners are becoming prevalent, and there are few studies assessing potential differences in volumetry between field strengths. More than 25% of ADNI subjects undergo both 1.5 Tesla and 3.0 Tesla MRI. Objectives: to compare ventricular measures derived from 1.5 Tesla and 3.0 Tesla MR scanners for ADNI subjects enrolled in the 3.0 Tesla MRI arm.

Baseline and 12-month data were selected from ADNI, which included 42 normal controls (NC) (mean age =76 years), 53 subjects with MCI (mean age =76 years) and 20 subjects with AD (mean age =76 years). Baseline and 12-month processed 3D T_1-weighted MP-RAGE MRI, and corresponding, demographic measures were collected. Ventricular volume was computed using a semi-automated region-growing algorithm (Cedara Software, Mississauga, Ontario). ICCs were computed to assess differences between 1.5 Tesla and 3.0 Tesla data for cross-sectional and longitudinal measures. A one-way ANOVA was used for group-wise comparisons between normal elderly controls (NEC), MCI and AD groups for baseline and longitudinal ventricular measures.

Ventricular volumes measured from 1.5 Tesla (mean ± SD: NEC = $31.5 \pm 11.2 cm^3$, MCI = 51.6 ± 23.9 cm^3, AD = 48.8 ± 26.5 cm^3) MRI strongly agreed with ventricular volumes derived from 3.0 Tesla MRI (NEC = 32.8 ± 11.2 cm^3, MCI = 53.8 ± 24.2 cm^3, AD = 49.8 ± $29.4cm^3$) at baseline (ICC = 0.99, CI (95%) = 0.96-0.99, $p<0.0001$). Ventricular

enlargement was moderately similar for measures derived from 1.5 Tesla MRI (mean ± SD = 2.6 ± 2.8 cm^3) and 3.0 Tesla MRI (mean ± SD = 2.5 ± 3.3 cm^3) when collapsing across groups (ICC = 0.75, CI (95%) = 0.66-0.82, p<0.0001). For both field strengths the AD and MCI groups had significantly greater ventricular enlargement after 12 months than the NC group (p<0.01).

These data demonstrate similar sensitivities for 1.5 Tesla and 3.0 Tesla derived ventricular measures. Baseline comparisons reveal high reproducibility between field strengths, with a slightly larger average ventricular volume for 3.0 Tesla measures. Moreover, ventricular enlargement was slightly larger for 1.5 Tesla measures in comparison to 3.0 Tesla measures. Despite these volumetric differences between field strengths, ventricular enlargement computed from 3.0 and 1.5 Tesla MRI demonstrated comparable group-wise discrimination.

3.2.2 CEREBRAL VENTRICULAR SUB-VOLUME ANALYSIS FROM MRI: A MARKER OF ALZHEIMER DISEASE PROGRESSION VALIDATED USING ADNI

Cerebral ventricular volume measured from MRI is an indirect global marker of AD progression (Jack, et al. 2004). Quantification of ventricular sub-regions may allow characterization of topographical disease progression and may also detect regional differences between NEC subjects with MCI and AD *in vivo* (Ferrarini, et al. 2008). These focal measures may provide greater sensitivity to disease progression than global measures of ventricular change. Objectives: To evaluate ventricle sub-region volume and enlargement between NEC, MCI, and AD groups.

Baseline and 12-month clinical and MRI data were obtained for 511 subjects (NEC=106; MCI=261; AD=124) from the Alzheimer Disease Neuroimaging Initiative database (complete listing available at www.loni.ucla.edu\ADNI\Collaboration\ADNI_Citation.shtml. 2007). Ventricular volume sub-region analysis was performed using BVQ (Cedara Software). BVQ segments the ventricles into 8 anatomical regions using highly reproducible anatomical rules. A method for segmenting the temporal horns was introduced in chapter 1. In brief, the posterior borders of the temporal horns were defined as the planes tangent to the left

and right trigones of the lateral ventricles. These planes approximately bisected the posterior inferior colliculus. Additional sub-volumes were segmented including the bilateral anterior horns, bodies of the ventricles and bilateral posterior horns (Figure 3-1). The border dividing the anterior horn and ventricular body was determined by the plain intersecting the anterior commissure. The plain dividing the ventricular body and posterior horn bisected the posterior commissure. A one-way ANOVA and Student-Newman-Keuls tests were used for group-wise comparisons. All volumes are reported as mean ± SD.

Figure 3-1 Three dimensionally rendered ventricular sub-volume segmentation. The ventricles are rendered in 3-D by Brain Ventricle Quantification software. A three dimensionally rendered superior to inferior view of this subject's ventricles is used to assess proper sub-volume segmentation. The anterior horns (AH), body (B), posterior cornu (PC) and temporal horns (TH) are visible for both hemispheres.

Baseline total (NEC = 1.5 ± 1.0 cm^3; MCI = 2.2 ± 1.5 cm^3; AD = 3.0 ± 2.0 cm^3) and bilateral temporal horn volumes were significantly different between all three groups (p <0.01). Total anterior horn volumes were greater for both the MCI (12.6 ± 7.6 cm^3) and AD groups (13.8 ± 8.4 cm^3) in comparison to NEC (11.0 ± 6.8 cm^3) (p <0.01). The AD group had a significantly greater total mid-body volume (14.9 ± 7.0 cm^3) than the MCI (13.4 ± 6.3 cm^3) and NEC groups (12.3 ± 5.7 cm^3) (p<0.01). All groups had significantly different total posterior horn volumes (NEC = 16.4 ± 9.6 cm^3; MCI = 20.5 ± 12.7 cm^3;

AD = 24.3 ± 15.0 cm^3) (p <0.01). Bilateral temporal horn enlargement was significantly greater for the AD group (0.3 ± 0.3 cm^3) than the MCI (0.2 ± 0.2 cm^3) and NEC groups (0.1 ± 0.2 cm^3) (p <0.01). Subjects with MCI had a greater average right temporal horn enlargement than NEC subjects (p <0.01).

Baseline volume and enlargement within the bilateral posterior cornus and temporal horns suggests marked atrophy occurs around the medial temporal lobe in MCI, and to a greater extent in AD in comparison to NEC. Persons with MCI had larger anterior horns than NEC, suggesting frontal lobe atrophy may occur in MCI. Cross-sectional and longitudinal measures of ventricular sub-regions reflect the topographical progression of AD *in vivo*.

3.3 IMPLICATIONS AND FUTURE WORK

This thesis interrogated ventricular enlargement in the healthy elderly, persons with MCI and persons with AD. Alzheimer disease is a neurodegenerative disease which leads to a loss in memory, functional abilities and leads to eventual death (Mosconi, et al. 2007). This disease is associated with soaring morbidity (Alzheimer's Society of Canada. January 2009, Vas, et al. 2001), and is associated with great emotional and financial costs to both individuals, families and to society (Mount and Downton. 2006). By using a novel region-growing algorithm BVQ described in chapter 1, it was demonstrated that persons with AD had significantly greater rates of ventricular enlargement than both NEC and MCI. The MCI group had a significantly greater rate of ventricular change in comparison to NEC. This finding validates the notion that structural MRI can be used to measure AD progression *in vivo*. Detecting differences in the rate of brain change between controls, MCI and AD may be useful in measuring disease progression in clinical trials of disease modifying therapies and contribute to an earlier diagnosis and prognosis of AD. This technique also confers a benefit of smaller subject samples to detect changes in brain tissue loss due to purported disease modifying therapies.

Although total ventricular volume provides a sensitive global measure of tissue change, certain issues arise from the use of this instrument in clinical samples. Although this method is sensitive to AD progression its specificity when applied to a variety of other

dementing illnesses to discriminate AD is unclear. A logical extension of this thesis would be to evaluate the specificity and sensitivity of ventricular volume to discriminate dementias such as frontotemporal dementia, Lewy body disease, vascular dementia, and AD. However, from the work of other authors it appears the utility of structural imaging alone yields modest specificities (de Leon, et al. 2004, de Leon, et al. 2006). A multimodal approach has been suggested to improve diagnostic specificity (Brys, et al. 2009, de Leon, et al. 2007). This is congruous with the new diagnostic research criteria suggested by Dubois *et al.* (Dubois, et al. 2007). By including MRI derived measures and serial measures of ventricular volume in conjunction with CSF protein samples and memory tests, a more accurate diagnosis may be rendered. An extension of this notion would be, therefore, to investigate the ability of CSF protein samples collected and banked in ADNI in combination with ventricular volumes to predict future cognitive decline. Another concern with using ventricular volume to measure AD progression is the changes in ventricular volume associated with normal pressure hydrocephalus (NPH) (Hurley, et al. 1999). Both NPH and AD are correlated with expanded ventricles and dementia. This may confound the specificity of ventricular volume as an independent diagnostic tool.

Another extension of the work in this thesis would be to validate ventricular enlargement as a surrogate endpoint for clinical trials. To test this hypothesis, ventricular volume could be implemented as a secondary endpoint retrospectively or ideally prospectively in a therapeutic trial of a purported disease modifying drug. Differences between placebo and control arms in terms of ventricular enlargement may help elucidate disease modification. However, the AN-1792 immunotherapy trial demonstrated increased ventricular enlargement in the treatment arm in comparison to controls (Fox NC. Black RS. Gilman S. Rossor MN. Griffith SG. Jenkins L. Koller M. AN1792(QS-21)-201 Study. 2005). However, these results are not definitive as the trial was suspended due to encephalitis in participants. Adequate follow-up is required to clearly understand tissue changes in AD immunotherapy trials. Further, it may be useful to include ventricular volume as a measure to select "responders" for clinical trials (van de Pol, et al. 2007). Hence, this optimizes the likelihood of detecting a treatment effect in comparison to the placebo group.

Sub-volumes of the ventricular CSF compartments may provide a focal measure of pathologic change. Specifically, measuring temporal horn volume changes is an attractive technique to indirectly measure MTL changes. It avoids the tissue contrast issues with hippocampal and parahippocampal structures (Giesel, et al. 2006) and further provides a rapid means to measure disease state. MTL structures according to Braak topological histopathology (Braak and Braak. 1994) are the first areas to demonstrate NFT pathology and precocious tissue atrophy. Moreover, other sub-regions may provide a marker of disease stage or provide a characteristic signature that may provide a differential diagnosis between dementing disorders (Ferrarini, et al. 2006, Ferrarini, et al. 2008). For instance, in FTD the frontal cortex is affected and becomes notably atrophic with sparing of the MTL (O'Brien. 2007). The frontal horn of the ventricles provides a means to measure deep frontal lobe changes and may discriminate between a person with MCI that will progress to AD and persons that will progress to clinical FTD.

Work in other neurodegenerative disorders may be useful such as Huntington's disease. This disease principally affects the caudate nuclei which are adjacent to the body and anterior horns of the lateral ventricles. Measuring disease progression in future neuroprotective therapeutic trials may provide a way of quantifying efficacy of neuronal sparing – similar to the approach with AD modifying therapeutic trials.

3.4 CONCLUSION

Alzheimer disease effects millions world-wide (Vas, et al. 2001) and developments in methods to characterize the disease progress *in vivo* provide a means to detect treatment effects and support an earlier diagnosis of AD. MRI is a non-destructive and non-invasive imaging modality that can provide exquisite anatomical brain images. In this thesis we have refined with Cedara Software the tool BVQ to semi-automatically compute the volume of the lateral ventricles in an accurate and precise manner. Moreover, we have demonstrated the potential of ventricular enlargement to measure disease progression over short intervals (<1 year). Future exploration and translation of this tool's capacity to complement other imaging modalities and CSF profiles may assist in an earlier prediction of progression to AD and may provide a method to detect treatment effects in disease modifying therapeutic trials.

3.5 REFERENCES

Alzheimer's Disease Neuroimaging Initiative
www.loni.ucla.edu\ADNI\Collaboration\ADNI_Citation.shtml. Alzheimer's
disease neuroimaging initiative (ADNI). 2007; 2007.

Alzheimer's Society of Canada. Alzheimer's disease fact sheet.
http://www.alzheimer.ca/english/media/adfacts2009.htm. January 2009; May
2009: 1.

Braak H, Braak E. Morphological criteria for the recognition of Alzheimer's disease
and the distribution pattern of cortical changes related to this disorder.
Neurobiol Aging 1994; 15: 355,6; 379-80.

Bradley KM, Bydder GM, Budge MM, Hajnal JV, White SJ, Ripley BD, et al. Serial
brain MRI at 3-6 month intervals as a surrogate marker for Alzheimer's
disease. Br J Radiol 2002; 75: 506-13.

Brys M, Glodzik L, Mosconi L, Switalski R, De Santi S, Pirraglia E, et al. Magnetic
resonance imaging improves cerebrospinal fluid biomarkers in the early
detection of Alzheimer's disease. J Alzheimer's Dis 2009; 16: 351-62.

Carmichael OT, Kuller LH, Lopez OL, Thompson PM, Dutton RA, Lu A, et al.
Ventricular volume and dementia progression in the cardiovascular health
study. Neurobiol Aging 2007; 28: 389-97.

de Leon MJ, DeSanti S, Zinkowski R, Mehta PD, Pratico D, Segal S, et al. MRI and
CSF studies in the early diagnosis of Alzheimer's disease. J Intern Med 2004;
256: 205-23.

de Leon MJ, Mosconi L, Blennow K, DeSanti S, Zinkowski R, Mehta PD, et al.
Imaging and CSF studies in the preclinical diagnosis of Alzheimer's disease.
Ann N Y Acad Sci 2007; 1097: 114-45.

de Leon MJ, DeSanti S, Zinkowski R, Mehta PD, Pratico D, Segal S, et al.
Longitudinal CSF and MRI biomarkers improve the diagnosis of mild
cognitive impairment. Neurobiol Aging 2006; 27: 394-401.

Dubois B, Feldman HH, Jacova C, Dekosky ST, Barberger-Gateau P, Cummings J, et
al. Research criteria for the diagnosis of Alzheimer's disease: Revising the
NINCDS-ADRDA criteria.[see comment]. Lancet Neurology 2007; 6: 734-46.

Ferrarini L, Palm WM, Olofsen H, van Buchem MA, Reiber JH, Admiraal-Behloul F.
Shape differences of the brain ventricles in Alzheimer's disease. Neuroimage
2006; 32: 1060-9.

Ferrarini L, Palm WM, Olofsen H, van der Landen R, Jan Blauw G, Westendorp RG,
et al. MMSE scores correlate with local ventricular enlargement in the

spectrum from cognitively normal to Alzheimer disease. *Neuroimage* 2008; 39: 1832-8.

Fox NC. Black RS. Gilman S. Rossor MN. Griffith SG. Jenkins L. Koller M. AN1792(QS-21)-201 Study. Effects of abeta immunization (AN1792) on MRI measures of cerebral volume in Alzheimer disease. *Neurology* 2005; 64: 1563-72.

Giesel FL, Hahn HK, Thomann PA, Widjaja E, Wignall E, von Tengg-Kobligk H, et al. Temporal horn index and volume of medial temporal lobe atrophy using a new semiautomated method for rapid and precise assessment. *AJNR Am J Neuroradiol* 2006; 27: 1454-8.

Hurley RA, Bradley WG,Jr, Latifi HT, Taber KH. Normal pressure hydrocephalus: Significance of MRI in a potentially treatable dementia. *Journal of Neuropsychiatry & Clinical Neurosciences* 1999; 11: 297-300.

Jack CR,Jr, Shiung MM, Gunter JL, O'Brien PC, Weigand SD, Knopman DS, et al. Comparison of different MRI brain atrophy rate measures with clinical disease progression in AD. *Neurology* 2004; 62: 591-600.

Mosconi L, Brys M, Glodzik-Sobanska L, De Santi S, Rusinek H, de Leon MJ. Early detection of Alzheimer's disease using neuroimaging. *Exp Gerontol* 2007; 42: 129-38.

Mount C, Downton C. Alzheimer disease: Progress or profit?. *Nat Med* 2006; 12: 780-4.

O'Brien JT. Role of imaging techniques in the diagnosis of dementia. *Br J Radiol* 2007; 80: S71-7.

Schott JM, Price SL, Frost C, Whitwell JL, Rossor MN, Fox NC. Measuring atrophy in Alzheimer disease: A serial MRI study over 6 and 12 months. *Neurology* 2005; 65: 119-24.

Silbert LC, Quinn JF, Moore MM, Corbridge E, Ball MJ, Murdoch G, et al. Changes in premorbid brain volume predict Alzheimer's disease pathology. *Neurology* 2003; 61: 487-92.

van de Pol LA, van der Flier WM, Korf ESC, Fox NC, Barkhof F, Scheltens P. Baseline predictors of rates of hippocampal atrophy in mild cognitive impairment. *Neurology* 2007; 69: 1491-7.

Vas CJ, Rajkumar S, Tanyakitipisal P, Chandra V. Alzheimer's disease: The brain killer, world health organization. 2001: 1-16.

Wang D, Chalk JB, Rose SE, de Zubicaray G, Cowin G, Galloway GJ, et al. MR image-based measurement of rates of change in volumes of brain structures. part II: Application to a study of Alzheimer's disease and normal aging. *Magn Reson Imaging* 2002; 20: 41-8.